Accepted Manuscript

Cyclic alpha-Conotoxin Peptidomimetic Chimeras as Potent GLP-1R Agonists

Joakim E. Swedberg, Christina I. Schroeder, Justin Mitchell, Thomas Durek, David P. Fairlie, David J. Edmonds, David A. Griffith, Roger B. Ruggeri, David R. Derksen, Paula M. Loria, Spiros Liras, David A. Price, David J. Craik

PII: S0223-5234(15)30230-0

DOI: 10.1016/j.ejmech.2015.08.046

Reference: EJMECH 8082

To appear in: *European Journal of Medicinal Chemistry*

Received Date: 6 May 2015

Revised Date: 18 August 2015

Accepted Date: 24 August 2015

Please cite this article as: J.E. Swedberg, C.I. Schroeder, J. Mitchell, T. Durek, D.P. Fairlie, D.J. Edmonds, D.A. Griffith, R.B. Ruggeri, D.R. Derksen, P.M. Loria, S. Liras, D.A. Price, D.J. Craik Cyclic alpha-Conotoxin Peptidomimetic Chimeras as Potent GLP-1R Agonists, *European Journal of Medicinal Chemistry* (2015), doi: 10.1016/j.ejmech.2015.08.046.

Cyclic alpha-Conotoxin Peptidomimetic Chimeras as Potent GLP-1R Agonists.

Joakim E. Swedberg[a], Christina I. Schroeder[a], Justin Mitchell[a], Thomas Durek[a], David P. Fairlie[a], David J. Edmonds[b], David A. Griffith[b], Roger B. Ruggeri[b], David R. Derksen[c], Paula M. Loria[c], Spiros Liras[b], David A. Price[b], and David J. Craik[a,*]

[a]Institute for Molecular Bioscience, The University of Queensland, Brisbane, 4072 QLD, Australia

[b]World Wide Medicinal Chemistry, CVMED, Pfizer Inc., Cambridge, Massachusetts, USA

[c]Pharmacokinetics, Dynamics and Metabolism, Worldwide Research & Development, Pfizer Inc., Groton, Connecticut, USA

*Corresponding author Address: Institute for Molecular Bioscience, The University of Queensland, Brisbane QLD 4072, Australia; Phone: +61 (0)7 3346 2019; Email: d.craik@imb.uq.edu.au.

HIGHLIGHTS

- Chimeras combining 11 residue peptidomimetics and α-conotoxins are potent GLP-1R agonists.
- Several chimeras had improved biophysical properties compared to the parent compounds.
- These bicyclic peptidomimetics provide a new avenue in the development of GLP-1R agonists.

ABBREVIATIONS

T2DM: type-2 diabetes mellitus, GLP-1R: glucagon-like peptide-1 receptor, GLP-1: glucagon-like peptide-1, GIP: glucose-dependent insulinotropic polypeptide, cAMP: cyclic adenosine monophosphate, HCTU: 2-(6-chloro-1H-benzotriazole-1-yl)-1,1,3,3 tetramethylaminium hexafluorophosphate, DIPEA: N,N-diisopropylethylamine, DMF: N,N-dimethylformamide, HATU: 1-[Bis(dimethylamino)methylene]-1H-1,2,3-triazolo[4,5-b]pyridinium 3-oxid hexafluorophosphate, R_g: radius of gyration, PSA: polar surface area, SA: surface area, vLogP: virtual log n-octanol/water partition coefficient.

GRAPHICAL ABSTRACT

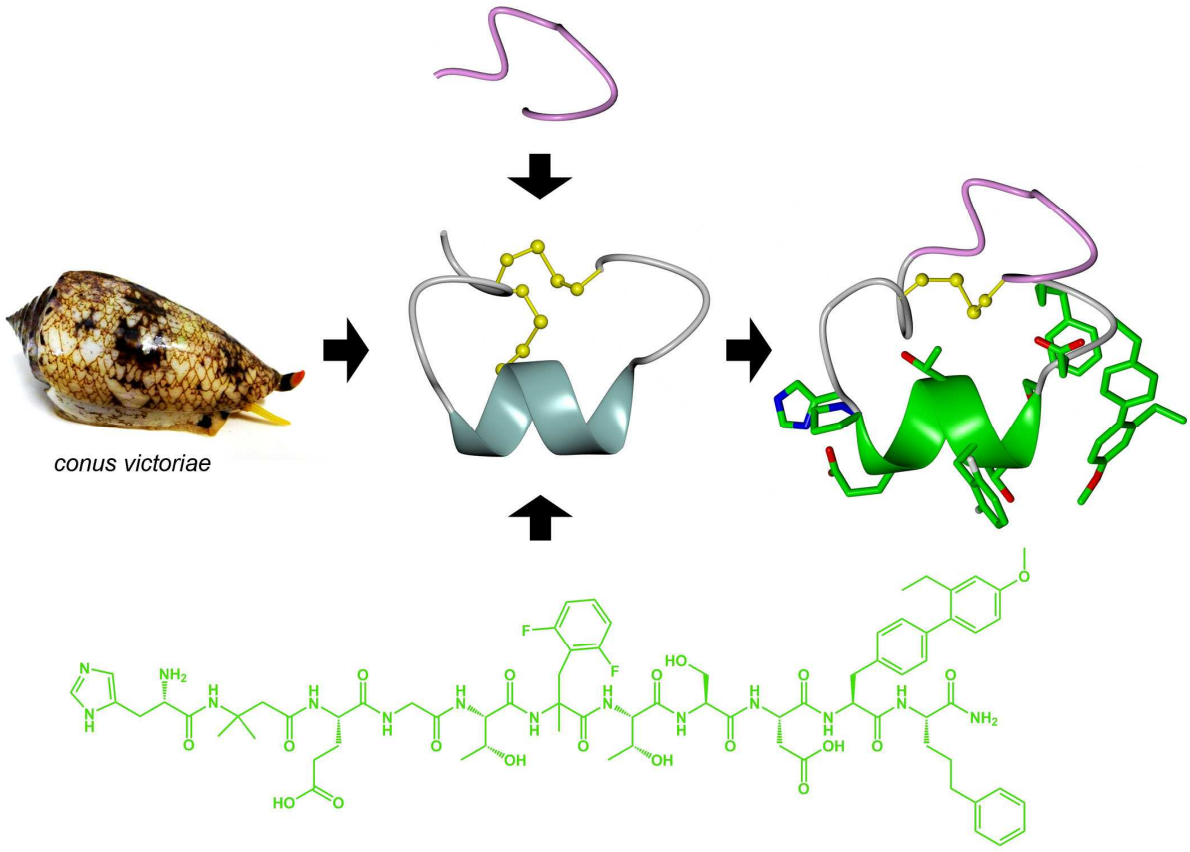

ABSTRACT

Type 2 diabetes mellitus (T2DM) results from compromised pancreatic β-cell function, reduced insulin production, and lowered insulin sensitivity in target organs resulting in hyperglycemia. The GLP-1 hormone has two biologically active forms, GLP-1-(7-37) and GLP-1-(7-36)amide, which are equipotent at the glucagon-like peptide-1 receptor (GLP-1R). These peptides are central both to normal glucose metabolism and dysregulation in T2DM. Several structurally modified GLP-1 analogues are now approved drugs, and a number of other analogues are in clinical trials. None of these compounds is orally bioavailable and all require parenteral delivery. Recently, a number of smaller peptidomimetics containing 11–12 natural and unnatural amino acids have been identified that have similar insulin regulating profiles as GLP-1. The α-conotoxins are a class of disulfide rich peptide venoms isolated from cone snails, and are known for their highly constrained structures and resistance to enzymatic degradation. In this study, we examined whether 11-residue peptidomimetics incorporated into α-conotoxin scaffolds, forming monocyclic or bicyclic compounds constrained by disulfide bonds and/or backbone cyclization, could activate the GLP-1 receptor (GLP-1R). Several compounds showed potent (nanomolar) agonist activity at GLP-1R, as evaluated via cAMP signaling. In addition, HPLC retention times and *in silico* calculations suggested that mono- and bicyclic compounds had more favorable n-octanol/water partition coefficients according to the virtual partition coefficient model (vLogP), while maintaining a smaller radius of gyration compared to corresponding uncyclized peptidomimetics. Our findings suggest that cyclic peptidomimetics provide a potential avenue for future design of potent, compact ligands targeting GLP-1R and possessing improved physicochemical properties.

KEYWORDS

Glucagon-like peptide-1; Exendin-4; Conotoxins; Glucagon-like peptide-1 Receptor; Type-2 diabetes mellitus.

INTRODUCTION

The rapid increase in the incidence of type 2 diabetes mellitus (T2DM) is resulting in a growing economic burden for health care systems globally. There are around 350 million diabetes sufferers [1] accounting for 6% of the total mortality rates worldwide [2], 90% of which are T2DM [3]. The cost associated with diabetes was over 376 billion USD in 2010 and is estimated to rise to 490 billion USD in 2030 [4]. Consequently, there is an urgent need for the development of new T2DM therapeutics with differentiation and improvement over those currently available.

T2DM is characterized by hyperglycemia resulting from compromised pancreatic β-cell function and reduced insulin production in conjunction with lowered insulin sensitivity in target organs [5]. Central to both the physiology of glucose metabolism and the pathophysiology of T2DM are the endogenously-produced incretin peptide hormones glucagon-like peptide-1 (GLP-1; Figure 1A) and glucose-dependent insulinotropic polypeptide (GIP) [6]. GLP-1 and GIP are secreted by cells lining the gastrointestinal tract in response to nutrient intake, and stimulate pancreatic β-cells to produce insulin. The incretins account for up to 70% of the prandial insulin response [7], and although both incretins are secreted at lower levels in T2DM patients, only GLP-1 retains its potent insulinotropic activity [8]. Consequently, GLP-1 or synthetic GLP-1 analogues have received considerable interest as leads for the development of T2DM therapeutics [9, 10]. GLP-1 is the product of posttranslational processing of the preproglucagon gene and is initially produced as GLP-1(1-37), before undergoing N-terminal truncation into the two equipotent products GLP-1(7-37) and GLP-1(7-36)-amide [11], hereafter described using the generic term 'GLP-1'.

The physiological effect of GLP-1 is not limited to insulin release, and includes inhibition of β-cell apoptosis, glucagon secretion, food intake and gastric emptying while promoting β-cell neogenesis, glucose disposal and cardiac function [7]. GLP-1 signaling primarily occurs through the G protein-coupled receptor, glucagon-like peptide-1 receptor (GLP-1R) [12]. GLP-1R signaling has been shown to involve multiple G protein-coupled pathways, including $G_{\alpha s}$, $G_{\alpha i}$, $G_{\alpha o}$ and $G_{\alpha q/11}$ [13, 14]. Most studies of pathways have measured $G_{\alpha s}$ coupling and increases in intracellular cAMP [15], protein kinase A and cAMP-regulated guanine nucleotide exchange factors [16]. Recent studies have also shown that (G-protein independent) β-arrestin-mediated pathways are important for downstream

modulation of the response to GLP-1 [17, 18]. It has become increasingly evident that GLP-1 achieves its biological effects through an exquisite balance between different signaling pathways, and to date no small-molecule GLP-1R agonists have accomplished this [19-22]. In contrast, a number of modified GLP-1 analogues have been shown to be as effective as GLP-1, and several are currently in clinical use or in clinical trials [9].

The first GLP-1R agonist to be approved for clinical use was exenatide (Byetta©), based on a GLP-1 analogue exendin-4 (Ex-4; Figure 1A) isolated from the saliva of the Gila monster (*H. suspectum*) [23]. GLP-1 shares 50% sequence identity with Ex-4, although the latter is a slightly more potent GLP-1R agonist than GLP-1 [24] and is more resistant to protease degradation *in vivo* [25]. Another approved GLP-1R agonist is liraglutide, a human GLP-1 analogue that has an added fatty acid moiety, which promotes albumin binding, improves circulation half-life, and confers resistance to protease degradation [26]. Agents currently available to T2DM patients need to be administrated subcutaneously either daily or weekly; however, a number of formulations based on GLP-1 or exenatide that allow dosing either one a week or month are currently in clinical trials [27]. Developing a GLP-1R agonist that is suitable for oral delivery is likely to increase patient compliance and is, therefore, highly desirable.

Recently an 11-amino acid peptidomimetic analogue based on the first nine residues of the N-terminus of GLP-1, with C-terminal biphenyl derivatives in position 10 and 11, was reported (BMS21; Figure 1B) [28]. BMS21 exhibited activity at low picomolar concentrations in cAMP signaling *in vitro* (EC_{50} = 0.087 ± 0.04 nM) and activity in an obese mouse model [28]. However, the signaling profile via various pathways *in vitro* is quite different to that of GLP-1, with a reduced G-protein-independent β-arrestin1/2-smediated response [29]. Additional work exploring variants of this peptide with substitutions at positions 10 and 11 led to the identification of a peptide where homo-homo-Phe replaced (2'-Me)-Biphenyl at position 11 in BMS21 (compound **1**; Figure 1B). This peptide displayed similar cAMP signaling activity *in vitro* and plasma glucose lowering activity *in vivo* as BMS21, but with a simplified route of synthesis [30, 31]. With the goal of obtaining an orally bioavailable variant, compound **13** was extended with Val N-terminally to target active transport by the PEPT1 transporter [32]. The resulting 12mer peptide (CYOG1) showed oral efficacy in several

preclinical diabetes models, including insulin release in ob/ob mice at similar levels to that of subcutaneous exenatide [33].

Peptide-based drugs typically have low bioavailability resulting from poor absorption across the gut wall, in conjunction with degradation by endogenous proteases in the digestive and circulatory systems. In general, disulfide-rich peptides are more resistant to chemical or enzymatic insult than unconstrained peptides. Conotoxins are such disulfide-rich peptides isolated from marine cone snail venoms that target nicotinic acetylcholine receptors. One such α-conotoxin, Vc1.1, isolated from the snail *Conus victoriae* [34], was found to activate $GABA_B$ receptors implicated in pain responses [35]. Recently an engineered cyclic variant of Vc1.1 (cVc1.1; Figure 1C) was shown to have oral efficacy in a rat model of neuropathic pain [36]. Another α-conotoxin, pc16a (Figure 1D), first isolated from the cone snail *Conus pictus* [37], shares several properties with GLP-1 and Ex-4: both classes of peptides have a flexible N-terminus followed by an α-helix, and target membrane receptors.

We recently reported a series of potent cyclic derivatives of **1** where the peptidomimetic was constrained by either lactam bridges between residues 5 and 9 or by disulfide bridges formed by cysteine analogues between residues 2 and 5 [38]. In this study, we produced a series of chimeric peptides by grafting BMS21/compound **1** analogues into mono- and bicyclic cVc1.1 and pc16a α-conotoxin frameworks. The resulting bicyclic peptides showed nanomolar to micromolar cAMP activity. This is the first report of such potent bicyclic peptidomimetics and provides a new avenue for exploring highly constrained cyclic GLP-1R agonists.

METHODS AND MATERIALS

Peptide Synthesis

Peptides were assembled on rink-amide (0.59 mmol/g; Chem-Impex) or 2-chlorotrityl resins (0.80 mmol/g; Chem-Impex) at a 0.25 mmol scale using Fmoc solid-phase peptide synthesis on a Symphony Multiplex Synthesizer. Fmoc-protected amino acids (4 eq.) were coupled using 4 eq. 2-(6-chloro-1H-benzotriazole-1-yl)-1,1,3,3 tetramethylaminium hexafluorophosphate (HCTU) and 8 eq. N,N-diisopropylethylamine (DIPEA) in N,N-dimethylformamide (DMF; 2 x 10 min). Fmoc deprotection was carried out using 30% piperidine in DMF (2 x 3 min). The following protecting

groups were used: Trt or acetamidomethyl (Acm) (Cys, His, Asn, and Gln), tBu (Asp, Glu, Ser, Thr, and Tyr), Boc (Lys and Trp), and Pbf (Arg).

Non-standard Fmoc amino acids were obtained from Chem-Impex International Inc. (Fmoc-*p*-phenyl-L-Phenylalanine and Fmoc-a-aminoisobutyric acid), ChemPep Inc. (Fmoc-S-trityl-L-penicillamine) and Alabiochem Tech. Co. Ltd (Fmoc-Abu-OH). (S)-2-(((9H-fluoren-9-yl)methoxy)carbonyl-amino)-3-(2'-ethyl-4'-methoxybiphenyl-4-yl)propanoic acid (Fmoc-Bip(2'-Et,4'-OMe)-OH), Fmoc-(S)-2-Fluoro-R-methylphenylalanine (α-Me-(2-F)-Phe) and Fmoc-(S)-2-6-difluoro-R-methylphenylalanine (α-Me-(2-6-di-F)-Phe were synthesized, as previously described [28]. Extended coupling times were used for the non-standard Fmoc protected amino acids: S-trityl-L-penicillamine ((β,β-di-Me)-Cys), (*S*)-2-amino-3-(2'ethyl-4-methoxy-[1,1'-biphenyl]4-yl)propanoic acid ((2'-Et, 4'-OMe)-BIP), (*S*)-2-amino-5-phenylpentanoic acid (hh-Phe), (*S*)-2-amino-2-methyl-3-phenylpropanoic acid (α-Me-Phe), (*S*)-2-amino-3-(2-fluorophenyl)propanoic acid (α-Me-(2-F)-Phe) and (*S*)-2-amino-3-(2,6-difluorophenyl)propanoic acid (α-Me-(2,6-di-F)-Phe). Non-standard Fmoc protected amino acids were coupled with 1.5 eq. amino acid, 1.5 eq. 1-[Bis(dimethylamino)methylene]-1H-1,2,3-triazolo[4,5-b]pyridinium 3-oxid hexafluorophosphate (HATU) and 3 eq. DIPEA for 1 h. Any amino acid following α-Me-Phe, α-Me-(2-F)-Phe and α-Me-(2,6-di-F)-Phe was particularly difficult and coupling was performed with 20 eq. amino acid, 20 eq. HATU and 40 eq. DIPEA for 18 h followed by standard 4 eq. amino acid, 4 eq. HCTU and 8 eq. DIPEA (3 x 1 h) and acetylation of unreacted sites. Assembled peptides were liberated from the resin and side chain deprotected using trifluoroacetic acid (TFA): triisopropylsilane: H_2O (95: 2.5: 2.5) over 2 h, before precipitation with ice-cold diethyl ether and lyophilization from acetonitrile/water mixtures containing 0.1% TFA.

Peptides were purified by HPLC (Shimadzu Prominence System) on a Phenomenex Jupiter 5µm (250 x 50 mm) column. Peptide purities (>95%) were confirmed using a Phenomenex Jupiter 5µm (150 x 2) mm column and peptide masses were determined by electrospray ionization MS (Shimadzu Prominence). Removal of the Cys Acm protecting groups and disulfide bond formation was achieved by dissolving peptide (0.5–1.0 mg/mL) in 80% aqueous acetic acid containing 1 mg/mL iodine. Alternatively, if the reaction proceeded slowly, acetic acid was substituted for methanol. The

reaction was monitored by MS, as described above, and was terminated by the addition of ascorbic acid until the iodine coloration disappeared. Correct disulfide bond folding was monitored by ^{1}H NMR (Figure S1).

CHO cAMP Accumulation Assay

CHO K1 cells stably transfected with hGLP-1R were grown at 37°C, 95% O_2 and 5% CO_2 in 75 cm flasks containing DMEM/F12 (1:1) media with added 1% GlutaMAX™ (Gibco®), 1% PenStrep and 1% Geneticin® (Gibco®) and grown until 90% confluent. Cells were then washed (PBS), lifted with cell dissociation solution (Sigma Aldrich), counted and used for cAMP accumulation assays and/or passaging (1:10). Following the manufacturer's instructions for the LANCE® Ultra cAMP assay (Perkin Elmer), cells transfected with hGLP-1R were centrifuged (1500 rpm, 5 min), re-suspended in cAMP assay buffer (HBSS, 5.56 mM glucose, 0.1% BSA, 0.5 mM IBMX, 5 mM HEPES), and seeded at 1000 cells per well in a ProxiPlate-384 Plus plate (Perkin Elmer). Cells were treated with compounds diluted in assay buffer over a range of concentrations (10 μM to 100 fM) and incubated for 30 min. Cell lysis buffers (Tracer (1:50) and Ulight (1:150)) were added to each well, and the places were incubated at room temperature for 2 h, before being read on a PHERAstar FS (BMG Labtech). Raw signals from three technical replicates were normalized as percentage of GLP-1 maximum before determining EC_{50} values using GraphPad Prism 6 from three independent experiments.

Molecular Modeling

The compounds were solvated in TIP3P water and 70% (v/v) dimethyl sulfoxide neutralized with Na^+/Cl^- counter ions using YASARA 13.9.8 [39] (systems consisted of 5000-6000 atoms, including 500–600 solvent molecules), and topologies were generated in VMD 1.9.2. Simulations were performed in NAMD 2.10 CUDA [40] with CHARMM27 force field parameters. Force field parameters for dimethyl sulfoxide and synthetic amino acids were constructed using CGenFF 2b8 [41] as a template, except for Aib (aa6) where SwissParam (http://www.swissparam.ch/) was used. Each system was equilibrated using a stepwise relaxation procedure under NPT (conserved substance (N),

pressure (P) and temperature (T)) conditions, as previously described [42]. The particle mesh Ewald algorithm was used to compute long-range electrostatic interactions at every time step and non-bonded interactions were truncated smoothly between 10.5 Å and 12 Å. All covalent hydrogen bonds were constrained by the SHAKE algorithm (or the SETTLE algorithm for water), permitting an integration time step of 2 fs. Three Production runs of 50 ns were performed for each compound under NVT (conserved substance (N), volume (V) and temperature (T)) conditions and coordinates were saved every 1000 simulation steps, producing 75000 total frames per compound.

Secondary structure analysis over time for compounds were calculated using the VMD timeline plugin (v2.3). Selection of the most representative structures from the simulation trajectories was based on backbone RMSD clustering in UCSF Chimera 1.8.1 [43], were the frame with the lowest RMSD relative to the largest cluster was selected. The radius of gyration, surface area and polar surface area were calculated from the molecular dynamics trajectories using VEGA ZZ 3.03 [44] and a water probe radius of 1.4 Å, and the n-octanol/water partitioning coefficients were calculated according the vLogP model [45].

RESULTS

Design and Agonist Activity of α-Conotoxin cVc1.1 Chimeras

There are currently no small molecule GLP-1R agonists with a similar activation profile to that of the endogenous agonist GLP-1 [29]. The smallest GLP-1R agonists with similar efficacy to GLP-1 are the 11-residue peptidomimetics, BMS21 and compound **1** (Figure 1B). BMS21 has a central 3_{10}-helical segment across residues 6–11 [28], and compound **1** was expected to have a similar conformation. Consequently, in our design process the sequence of **1** with the substitution Aib2 (aa6) to Pro2 was grafted into the helical segment of the engineered cyclotide cVc1.1 [36] (Figure 1C), to produce both open **2** and backbone cyclic **3** grafted peptidomimetics. The Aib2 residue in **1** was substituted for Pro2 because this residue is important for maintaining the fold of cVc1.1 [46] (Figure 1C and 1E; Table 1). Comparing GLP-1R activation for the linear starting compound **1** with the monocyclic compound **2** indicated a 6-fold reduction in cAMP signaling (Table 2). Backbone cyclization of **2** produced bicyclic compound **3**, which was accompanied by a 500-fold reduction in cAMP activity. To confirm

that Aib2 present in **1** was not suitable for the cyclotide cVc1.1 scaffold, Pro2 in **3** was substituted for Aib2 to produce **4**, which was accompanied by >3-fold reduction in potency of cAMP signaling.

To investigate if the reduction in potency, resulting from backbone cyclization of **2** to **3**, related to loss of the N-terminal amine or loss of flexibility, **2** was acetylated at the N-terminus. The resulting compound **5** was found to have intermediate cAMP potency compared to **2** and **3**, suggesting that both a free N-terminus and N-terminal flexibility are important for receptor activation. During the optimization of BMS21 it was found that the 2,6-di-fluorine substitution of α-Me-Phe6 (aa10) was a marginally more potent cAMP activator than the 2-mono-flourine derivative (aa9) [28]. The same substitution in **2** to produce **6** had a similar marginal effect on cAMP signaling.

Backbone cyclization of **6** to **7** resulted in a larger (>2-fold) loss of cAMP activity. Substituting α-Me-(2-F)-Phe2 (aa9) in **7** with α-Me-Phe2 (aa8) in **8** caused a further 2-fold reduction in cAMP signaling. Interestingly, substituting the α-Me-Phe2 in **8** with Phe2 in **9** was accompanied by a 5-fold recovery of cAMP potency, suggesting that there was interdependency between the α-Me group and the fluorine(s) in promoting potency.

Subsequently, we wanted to investigate the possibility of increasing the hydrophobicity of **2** and **3** by modifying the cyclization linker in cVc1.1. Residues 15–17 and 19–20 were substituted with Val residues in the mono- and bicyclic compounds **10** and **11**. However, these substitutions were accompanied by a 20-fold and 2-fold reduction of cAMP signaling, respectively. Similarly, residues 15–20 in **2** and **3** were also substituted for Leu residues, but in conjunction with α-Me-(2-F)-Phe2 to α-Me-Phe2 substitutions, to produce compounds **12** and **13,** respectively. The rational for the residue 2 substitution was that this substitution in **8** resulted in a slight improvement in cAMP activity; however, both **12** and **13** were found to have reduced cAMP potency.

Considering the importance of the biphenyl derivatives in positions 10–11 of BMS21 for cAMP activity [28], Gly14 in the cVc1.1 linker of **2** and **3** was substituted for biphenyl to give compounds **14** and **15**. These substitutions were well tolerated and only resulted in minor (1.1–2.8-fold) losses of cAMP signaling potency. Compounds **14** and **15** were then substituted with α-Me-Phe at position 2 to produce **16** and **17**, respectively. These substitutions had different consequences for the mono- and bicyclic compounds, with the former losing activity and the latter gaining activity. This

trend is similar to that seen for **8**, where the α-Me-Phe substitution at position 2 was favorable, and it appears that the bicyclic form of α-Me-Phe2 is more effective than α-Me-(2-F)-Phe2. By grafting compound **1** into cVc1.1, additional constraints were introduced by the presence of a disulfide bond. To investigate the effect of further increasing these constraints, Cys12 and Cys21 in **2** and **3** were substituted with (β,β-di-Me)-Cys (aa7) to produce **18** and **19**, and these changes were accompanied by 3–5-fold reductions in cAMP signaling. Thus, it appears that the disulfide bond constraint had a negative effect on potency. Consequently, Cys12 and Cys21 were substituted with Abu12 and Abu21 (aa5) in the most potent variant, compound 2. The resulting compound 20 showed a 2-fold increase in potency of cAMP signaling and became the most potent variant.

Design and Agonist Activity of α-Conotoxin pc16a Chimeras

For the cVc1.1 grafted variants, the sequence of **1** was uninterrupted by disulfide bonds, and thus we wanted to examine the possibility of constraining the peptidomimetic further by introducing disulfide bonds within the actual sequence of **1** using the non-cyclic α-conotoxin pc16a. Grafting **1** into pc16a resulted in **21**, where Thr_5 and Thr_7 were substituted with Cys residues designed to form a disulfide bond. Compound **21** showed a 3000-fold reduction in cAMP activity. Interestingly, the two bicyclic compounds, **3** and **21**, showed an equal loss of agonist activity irrespective of the scaffold. Further substitution of α-Me-(2,6-di-fluorine)-Phe6 with α-Me-(2-fluorine)-Phe6 and α-Me-Phe6 in **21** to give compounds **22** and **23** was accompanied by a further 12- and 4-fold reduction in cAMP signaling potency, respectively, which is more than for the same substitutions in **7**. Furthermore, substituting α-Me-(2-fluorine)-Phe6 in **23** for Phe6 resulted in **24** and a further 10-fold reduction in cAMP signaling potency, a substitution that had a 5-fold positive effect for the comparable substitution in **8**. Interestingly, N-terminal acetylation of **21** to give compound **25** caused a 6-fold increase in potency, which is the opposite effect seen for the equivalent addition to compound **2**, which lost 15-fold in potency. In compound **21**, Leu12 remained from the pc16a scaffold without known function, and was substituted for a biphenyl residue, but the resulting compound **26** showed a 17-fold reduction in cAMP signaling.

Molecular Modeling of α-Conotoxin Chimeras

To gain insight into how grafting of the peptidomimetics into α-conotoxins affected their structure, selected grafted variants were subjected to 150 ns (3 x 50 ns) molecular dynamics simulations. Since NMR spectroscopy studies of BMS21 in 70:30 dimethyl sulfoxide:water have been previously reported [28], the same solvent system was used for the simulations. However, since the atomic coordinates of the BMS21 structure have not been released, a comparison could only be based on the published description. BMS21 was found to adopt a 3_{10}-helix spanning residues 6–11 (with residues 9–11 being distorted from the canonical conformation) and a distorted type I turn or type VIIa turn across residues 2–4 with a kink at Aib2.

The model of compound **1** was suggested to have an α-helix spanning residues 3–8 during the majority of the simulation trajectory and random coil conformations for residues 9–11 and 1–2, with a distinct kink at Aib2 as for BMS21 (Figure 2A and Figure S2). The monocyclic compound **2** model was nearly identical to **1** across residues 3–10 (Cα RMSD: 0.93 Å), with a α-helix spanning residues 3–9, although residues 1–2 were more extended and lacked the residue 2 kink (Figure 2B and Figure S2). Similarly, the model of the bicyclic compound **3** overlaid closely across residues 3–10 with **1** (Cα RMSD: 1.06 Å) and **2** (Cα RMSD: 1.11 Å) and displayed comparable structural features across the N-terminal 11 residue segment (Figure 2C and Figure S2). Aligning the models of compound **10** and **11** (Figure 2D and Figure S2) with **1** indicated a strikingly close alignment across residues 3-9 (Cα RMSD: 0.32 Å and 0.22 Å respectively). However, both the peptide backbone and side chains of residues 10-11 deviated greatly from compounds **1-3** which may explain the dramatic loss of cAMP activity for these variants. The modeled structure of compound **20** differed greatly from the other structures with the lack of any cyclic constraints resulting in mostly a turn motif across the whole peptide, with some intermittent 3_{10}-helix/α-helix tendency across residues 11-13. Compound **21**, which was based on a different α-conotoxin scaffold (pc16a) compared to compounds **2-20** (Vc1.1), also appeared structurally different with a 3_{10} helical tendency across residues 2-4 with a turn motif across residues 6-10 (Figure 2E and Figure S2).

Although **2** and **3** contain twice as many amino acids as **1** and have masses 50% larger than **1**, both had smaller radii of gyration (R_g; Table 3). The additional amino acids in **2** and **3** resulted in noticeable increases in surface area (SA), polar surface area (PSA), and a lower n-octanol/water partition coefficient according to the vLogP model [45]. Introducing Val residues in the Ala-Gly linker of **2** and **3** to produce **10** and **11** reduced the PSA and greatly increased the lipophilicity, as indicated by the vLogP values. The most potent variant, the non-cyclic compound **20**, had the least favorable biophysical properties with the largest R_g, PSA and SA, and the lowest vLOGp. Compounds **21** and **25**, with three more amino acids and a mass ~20% larger than **1**, had the smallest R_g of the peptides examined. Compound **25**, the most potent cAMP agonist based on the pc16a scaffold, had a PSA comparable to **1**, but with greatly increased lipophilicity as indicated by the vLogP.

Perfluorophenylene-Crosslinked Compound 1 Analogues

To further increase hydrophobicity and potentially membrane permeability while maintaining α-helicity in the C-terminal part (residues 6–11) of the parent molecule, we designed a series of stapled compound **1** analogues based on a recently developed cysteine perfluoroarylation approach [47]. Previously reported [38] structure-activity data for pharmacophore (**1**) suggest that substitution of Thr5, Thr7 and Asp9 as well as C-terminal extensions [32] are well tolerated and may yield molecules that retain potent GLP1R activation. Pairs of cysteines were introduced in an i, i+4 configuration in positions 5/9 (**27**) and 8/12 (**28**) and were cross-linked by reaction with hexafluorobenzene under mild conditions in solution, as previously reported (Figure 3). Similarly, compound **29**, containing a perfluorobiphenyl staple (designed to span two α-helical turns), was generated by introducing cysteines in positions 5 and 12 (i, i+7) and reaction of the unprotected peptide with decafluorobiphenyl. The resulting molecules displayed a large shift to later RP-HPLC retention times compared to the non-stapled parent molecules, suggesting significantly increased hydrophobicity and reduced PSA. This was confirmed by MD simulations where, for example, **27** had the smallest R_g, PSA and SA as well as the highest vLogP of all compounds investigated (Table 3). The modeled structure of **27** overlaid very closely with compound **1** across residues 3–9 (Cα RMSD 0.62); however, the increased N-terminal and C-terminal helicity of **27** resulted in that residues 1–2 and 9–

11 deviated greatly from **1** in both backbone conformation and spatial side chain orientation (Figure 2F and Figure S2), which may account for the reduced cAMP activity.

CONCLUSIONS

This study has demonstrated that it is possible to produce bicyclic peptidomimetic GLP-1R agonists that maintain potent cAMP activity. By capitalizing on cyclization patterns optimized through evolution to maintain certain secondary structure motifs in naturally occurring disulfide-rich α-conotoxins, these motifs were maintained in the cyclic peptidomimetic chimeras. The consequences of cyclization often included a reduction of the radius of gyration while increasing the overall lipophilicity, characteristics frequently associated with improved membrane permeability and bioavailability [48]. These findings open up new avenues for the design of potent bicyclic GLP-1R agonists.

It is interesting that, in the process of grafting smaller peptidomimetics into larger cyclic peptide scaffolds, the radius of gyration can be reduced, which appears to be a direct result of the additional constraints induced by cyclization. The values estimated for the radius of gyration of grafted cVc1.1 variants by molecular dynamics correspond well to that previously determined for wild-type cVc1.1 using pulsed-field gradient NMR (R_g = 7.45 Å [49]). Other consequences of this are both masking of the polar termini, and that hydrophobic residues are locked in conformations exposing them to the solvent, resulting in increased molecular hydrophobicity.

An additional beneficial effect of cyclization is stabilization, leading to increased resistance to chemical, thermal or enzymatic insult; indeed, a number of backbone-cyclized conotoxins have been reported to share these properties [50-52]. This is also true for cyclotides, a class of plant-derived disulfide-rich and backbone-cyclized peptides [53, 54]. Recently bioactive peptides were grafted into the cyclotide kalata B1 scaffold to produce bradykinin B1 receptor antagonists for inflammatory pain treatment, and these were shown to have an analgesic effect after oral administration in mice [55]. Similarly, an engineered cyclic version of Vc1.1 (the framework used in the current study) was found to have oral efficacy in a rat model of neuropathic pain [36].

It appears that cyclization through disulfide bonds within the sequence of **1** was much better tolerated than backbone cyclization; undeniably, all compounds that were cyclized through their backbone lost potency for cAMP signaling. At the same, time both disulfide and backbone cyclization appeared to have beneficial effects by reducing the radius of gyration, PSA and SA while increasing the molecular lipophilicity. Compound **20** showed the most potent cAMP signaling and yet was linear, but at the same time was estimated to have the least favorable biophysical properties for drug delivery. This suggests the possibility for temporary constraint of compound **20** in a mono- or bicyclic pro-drug having properties that initially are similar to **2** or **3**. There are a number of approaches available for introducing temporary bonds that undergo chemical or enzymatic cleavage *in vivo* to release the active parent molecule. For example, ester bonds that are cleaved *in vivo* by esterases have been used to produce a number of successful pro-drugs with improved lipophilicity, permeability and bioavailability [56].

We have previously shown that monocyclic analogues of **1** can be potent GLP-1R agonists [38]. In this study we have demonstrated that it is possible to produce bicyclic, and even more highly constrained, potent peptidomimetic GLP-1R agonists. Further studies of potential cyclization points and various substituents are needed to find compounds with properties even more conducive for increased lipophilicity and permeability, while maintaining potent GLP-1R signaling. Additionally, these compounds need further evaluation to ensure that the exquisite balance between the various intracellular signaling pathways is maintained. These highly constrained bicyclic peptidomimetics may provide an exciting new therapeutic avenue towards the development of GLP-1R agonists with improved oral bioavailability properties.

ACKNOWLEDGMENTS

This work was supported in part by an Australian Research Council Linkage grant (LP110200213), a Queensland Government Department of Science, Information Technology, Innovation and the Arts Co-investment Fund grant, and a grant from Pfizer, Inc. DJC and DPF are National Health and Medical Research Council (NHMRC) Professorial Fellows (APP1026501 and APP1027369), JES is an NHMRC Early Career Fellow (APP1069819).

CONFLICT OF INTEREST

The authors declare that there is no conflict of interest.

AUTHOR CONTRIBUTIONS

JES designed the peptides, planned experiments, performed *in silico* calculations and drafted the manuscript. JM performed the cAMP assays. TD synthesized the perfluorophenylene-crosslinked compounds and drafted the manuscript. CIS, DPF, DJE, DAG, RBR, DRD PML, SL, DAP and DJC planned experiments, analyzed data and drafted the manuscript. All authors have approved the final article.

REFERENCES

1. G. Danaei; M. M. Finucane; Y. Lu; G. M. Singh; M. J. Cowan; C. J. Paciorek; J. K. Lin; F. Farzadfar; Y. H. Khang; G. A. Stevens; M. Rao; M. K. Ali; L. M. Riley; C. A. Robinson; M. Ezzati, National, regional, and global trends in fasting plasma glucose and diabetes prevalence since 1980: systematic analysis of health examination surveys and epidemiological studies with 370 country-years and 2.7 million participants. Lancet 378 (2011) 31-40.

2. World Health Organization, Global health risks: mortality and burden of disease attributable to selected major risks. World Health Organization: Geneva, 2009; p 17.

3. K. G. Alberti; P. Z. Zimmet, Definition, diagnosis and classification of diabetes mellitus and its complications. Part 1: diagnosis and classification of diabetes mellitus provisional report of a WHO consultation. Diabet Med 15 (1998) 539-53.

4. P. Zhang; X. Zhang; J. Brown; D. Vistisen; R. Sicree; J. Shaw; G. Nichols, Global healthcare expenditure on diabetes for 2010 and 2030. Diabetes Res Clin Pract 87 (2010) 293-301.

5. S. E. Kahn; M. E. Cooper; S. Del Prato, Pathophysiology and treatment of type 2 diabetes: perspectives on the past, present, and future. Lancet 383 (2014) 1068-83.

6. S. A. Ross; E. A. Gulve; M. Wang, Chemistry and biochemistry of type 2 diabetes. Chem Rev 104 (2004) 1255-82.

7. L. L. Baggio; D. J. Drucker, Biology of incretins: GLP-1 and GIP. Gastroenterology 132 (2007) 2131-57.

8. M. A. Nauck; M. M. Heimesaat; C. Orskov; J. J. Holst; R. Ebert; W. Creutzfeldt, Preserved incretin activity of glucagon-like peptide 1 [7-36 amide] but not of synthetic human gastric inhibitory polypeptide in patients with type-2 diabetes mellitus. J Clin Invest 91 (1993) 301-7.

9. M. Lorenz; A. Evers; M. Wagner, Recent progress and future options in the development of GLP-1 receptor agonists for the treatment of diabesity. Bioorg Med Chem Lett 23 (2013) 4011-8.

10. B. Manandhar; J. M. Ahn, Glucagon-like peptide-1 (GLP-1) analogs: recent advances, new possibilities, and therapeutic implications. J Med Chem 58 (2015) 1020-37.

11. C. Orskov; A. Wettergren; J. J. Holst, Biological effects and metabolic rates of glucagonlike peptide-1 7-36 amide and glucagonlike peptide-1 7-37 in healthy subjects are indistinguishable. Diabetes 42 (1993) 658-61.

12. G. V. Segre; S. R. Goldring, Receptors for secretin, calcitonin, parathyroid hormone (PTH)/PTH-related peptide, vasoactive intestinal peptide, glucagonlike peptide 1, growth hormone-releasing hormone, and glucagon belong to a newly discovered G-protein-linked receptor family. Trends Endocrinol Metab 4 (1993) 309-14.

13. M. Hallbrink; T. Holmqvist; M. Olsson; C. G. Ostenson; S. Efendic; U. Langel, Different domains in the third intracellular loop of the GLP-1 receptor are responsible for Galpha(s) and Galpha(i)/Galpha(o) activation. Biochim Biophys Acta 1546 (2001) 79-86.

14. C. Montrose-Rafizadeh; P. Avdonin; M. J. Garant; B. D. Rodgers; S. Kole; H. Yang; M. A. Levine; W. Schwindinger; M. Bernier, Pancreatic glucagon-like peptide-1 receptor couples to multiple G proteins and activates mitogen-activated protein kinase pathways in Chinese hamster ovary cells. Endocrinology 140 (1999) 1132-40.

15. D. J. Drucker; J. Philippe; S. Mojsov; W. L. Chick; J. F. Habener, Glucagon-like peptide I stimulates insulin gene expression and increases cyclic AMP levels in a rat islet cell line. Proc Natl Acad Sci U S A 84 (1987) 3434-8.

16. G. G. Holz, Epac: A new cAMP-binding protein in support of glucagon-like peptide-1 receptor-mediated signal transduction in the pancreatic beta-cell. Diabetes 53 (2004) 5-13.

17. N. Sonoda; T. Imamura; T. Yoshizaki; J. L. Babendure; J. C. Lu; J. M. Olefsky, Beta-Arrestin-1 mediates glucagon-like peptide-1 signaling to insulin secretion in cultured pancreatic beta cells. Proc Natl Acad Sci U S A 105 (2008) 6614-9.

18. J. Quoyer; C. Longuet; C. Broca; N. Linck; S. Costes; E. Varin; J. Bockaert; G. Bertrand; S. Dalle, GLP-1 mediates antiapoptotic effect by phosphorylating Bad through a beta-arrestin 1-mediated ERK1/2 activation in pancreatic beta-cells. J Biol Chem 285 (2010) 1989-2002.

19. C. Koole; K. Pabreja; E. E. Savage; D. Wootten; S. G. Furness; L. J. Miller; A. Christopoulos; P. M. Sexton, Recent advances in understanding GLP-1R (glucagon-like peptide-1 receptor) function. Biochem Soc Trans 41 (2013) 172-9.

20. C. Koole; E. E. Savage; A. Christopoulos; L. J. Miller; P. M. Sexton; D. Wootten, Minireview: Signal bias, allosterism, and polymorphic variation at the GLP-1R: implications for drug discovery. Mol Endocrinol 27 (2013) 1234-44.

21. F. S. Willard; A. B. Bueno; K. W. Sloop, Small molecule drug discovery at the glucagon-like peptide-1 receptor. Exp Diabetes Res 2012 (2012) Article ID: 709893.

22. F. S. Willard; K. W. Sloop, Physiology and emerging biochemistry of the glucagon-like peptide-1 receptor. Exp Diabetes Res 2012 (2012) Article ID: 470851.

23. J. Eng; W. A. Kleinman; L. Singh; G. Singh; J. P. Raufman, Isolation and characterization of exendin-4, an exendin-3 analogue, from Heloderma suspectum venom. Further evidence for an exendin receptor on dispersed acini from guinea pig pancreas. J Biol Chem 267 (1992) 7402-5.

24. D. Donnelly, The structure and function of the glucagon-like peptide-1 receptor and its ligands. Br J Pharmacol 166 (2012) 27-41.

25. R. Cvetković; G. Plosker, Exenatide. Drugs 67 (2007) 935-954.

26. C. Perry, Liraglutide. Drugs 71 (2011) 2347-2373.

27. S. L. Samson; A. Garber, GLP-1R agonist therapy for diabetes: benefits and potential risks. Curr Opin Endocrinol Diabetes Obes 20 (2013) 87-97.

28. C. Mapelli; S. I. Natarajan; J. P. Meyer; M. M. Bastos; M. S. Bernatowicz; V. G. Lee; J. Pluscec; D. J. Riexinger; E. S. Sieber-McMaster; K. L. Constantine; C. A. Smith-Monroy; R. Golla; Z. Ma; D. A. Longhi; D. Shi; L. Xin; J. R. Taylor; B. Koplowitz; C. L. Chi; A. Khanna; G. W. Robinson; R. Seethala; I. A. Antal-Zimanyi; R. H. Stoffel; S. Han; J. M. Whaley; C. S. Huang; J. Krupinski; W. R. Ewing, Eleven amino acid glucagon-like peptide-1 receptor agonists with antidiabetic activity. J Med Chem 52 (2009) 7788-99.

29. D. Wootten; E. E. Savage; F. S. Willard; A. B. Bueno; K. W. Sloop; A. Christopoulos; P. M. Sexton, Differential activation and modulation of the glucagon-like peptide-1 receptor by small molecule ligands. Mol Pharmacol 83 (2013) 822-34.

30. T. S. Haque; V. G. Lee; D. Riexinger; M. Lei; S. Malmstrom; L. Xin; S. Han; C. Mapelli; C. B. Cooper; G. Zhang; W. R. Ewing; J. Krupinski, Identification of potent 11mer glucagon-like

peptide-1 receptor agonist peptides with novel C-terminal amino acids: Homohomophenylalanine analogs. Peptides 31 (2010) 950-5.

31. T. S. Haque; R. L. Martinez; V. G. Lee; D. G. Riexinger; M. Lei; M. Feng; B. Koplowitz; C. Mapelli; C. B. Cooper; G. Zhang; C. Huang; W. R. Ewing; J. Krupinski, Exploration of structure-activity relationships at the two C-terminal residues of potent 11mer Glucagon-Like Peptide-1 receptor agonist peptides via parallel synthesis. Peptides 31 (2010) 1353-60.

32. R. Bahekar; M. R. Jain; P. R. Patel Short chain peptidomimetics based orally active glp-1 agonist and glucagon receptor antagonist. WO 2011/048614 A2, 2011.

33. D. J. Edmonds; D. A. Price, Oral GLP-1 Modulators for the Treatment of Diabetes. Annual Reports in Medicinal Chemistry 48 (2013) 119-130.

34. D. W. Sandall; N. Satkunanathan; D. A. Keays; M. A. Polidano; X. Liping; V. Pham; J. G. Down; Z. Khalil; B. G. Livett; K. R. Gayler, A novel alpha-conotoxin identified by gene sequencing is active in suppressing the vascular response to selective stimulation of sensory nerves in vivo. Biochemistry 42 (2003) 6904-11.

35. B. Callaghan; A. Haythornthwaite; G. Berecki; R. J. Clark; D. J. Craik; D. J. Adams, Analgesic alpha-conotoxins Vc1.1 and Rg1A inhibit N-type calcium channels in rat sensory neurons via GABAB receptor activation. J Neurosci 28 (2008) 10943-51.

36. R. J. Clark; J. Jensen; S. T. Nevin; B. P. Callaghan; D. J. Adams; D. J. Craik, The engineering of an orally active conotoxin for the treatment of neuropathic pain. Angew Chem Int Ed Engl 49 (2010) 6545-8.

37. A. Van Der Haegen; S. Peigneur; N. Dyubankova; C. Moller; F. Mari; E. Diego-Garcia; R. Naude; E. Lescrinier; P. Herdewijn; J. Tytgat, Pc16a, the first characterized peptide from Conus pictus venom, shows a novel disulfide connectivity. Peptides 34 (2012) 106-13.

38. H. N. Hoang; K. Song; T. A. Hill; D. R. Derksen; D. J. Edmonds; W. M. Kok; C. Limberakis; S. Liras; P. M. Loria; V. Mascitti; A. M. Mathiowetz; J. M. Mitchell; D. W. Piotrowski; D. A. Price; R. V. Stanton; J. Y. Suen; J. M. Withka; D. A. Griffith; D. P. Fairlie, Short Hydrophobic Peptides with Cyclic Constraints Are Potent Glucagon-like Peptide-1 Receptor (GLP-1R) Agonists. J Med Chem (2015).

513 39. E. Krieger; G. Koraimann; G. Vriend, Increasing the precision of comparative models with
514 YASARA NOVA--a self-parameterizing force field. Proteins 47 (2002) 393-402.
515 40. J. C. Phillips; R. Braun; W. Wang; J. Gumbart; E. Tajkhorshid; E. Villa; C. Chipot; R. D.
516 Skeel; L. Kale; K. Schulten, Scalable molecular dynamics with NAMD. J Comput Chem 26 (2005)
517 1781-802.
518 41. K. Vanommeslaeghe; E. Hatcher; C. Acharya; S. Kundu; S. Zhong; J. Shim; E. Darian; O.
519 Guvench; P. Lopes; I. Vorobyov; A. D. Mackerell, Jr., CHARMM general force field: A force field
520 for drug-like molecules compatible with the CHARMM all-atom additive biological force fields. J
521 Comput Chem 31 (2010) 671-90.
522 42. J. E. Swedberg; S. J. de Veer; K. C. Sit; C. F. Reboul; A. M. Buckle; J. M. Harris, Mastering
523 the canonical loop of serine protease inhibitors: enhancing potency by optimising the internal
524 hydrogen bond network. PLoS One 6 (2011) e19302.
525 43. E. F. Pettersen; T. D. Goddard; C. C. Huang; G. S. Couch; D. M. Greenblatt; E. C. Meng; T.
526 E. Ferrin, UCSF Chimera--a visualization system for exploratory research and analysis. J Comput
527 Chem 25 (2004) 1605-12.
528 44. A. Pedretti; L. Villa; G. Vistoli, VEGA--an open platform to develop chemo-bio-informatics
529 applications, using plug-in architecture and script programming. J Comput Aided Mol Des 18 (2004)
530 167-73.
531 45. V. K. Gombar; K. Enslein, Assessment of n-octanol/water partition coefficient: when is the
532 assessment reliable? J Chem Inf Comput Sci 36 (1996) 1127-34.
533 46. R. Halai; R. J. Clark; S. T. Nevin; J. E. Jensen; D. J. Adams; D. J. Craik, Scanning
534 mutagenesis of alpha-conotoxin Vc1.1 reveals residues crucial for activity at the alpha9alpha10
535 nicotinic acetylcholine receptor. J Biol Chem 284 (2009) 20275-84.
536 47. A. M. Spokoyny; Y. Zou; J. J. Ling; H. Yu; Y. S. Lin; B. L. Pentelute, A perfluoroaryl-
537 cysteine S(N)Ar chemistry approach to unprotected peptide stapling. J Am Chem Soc 135 (2013)
538 5946-9.

539 48. M. J. Waring, Defining optimum lipophilicity and molecular weight ranges for drug
540 candidates-Molecular weight dependent lower logD limits based on permeability. Bioorg Med Chem
541 Lett 19 (2009) 2844-51.
542 49. C. K. Wang; S. E. Northfield; J. E. Swedberg; P. J. Harvey; A. M. Mathiowetz; D. A. Price;
543 S. Liras; D. J. Craik, Translational diffusion of cyclic peptides measured using pulsed-field gradient
544 NMR. J Phys Chem B 118 (2014) 11129-36.
545 50. R. J. Clark; D. J. Craik, Engineering cyclic peptide toxins. Methods Enzymol 503 (2012) 57-
546 74.
547 51. R. J. Clark; M. Akcan; Q. Kaas; N. L. Daly; D. J. Craik, Cyclization of conotoxins to improve
548 their biopharmaceutical properties. Toxicon 59 (2012) 446-55.
549 52. C. I. Schroeder; D. J. Craik, Therapeutic potential of conopeptides. Future Med Chem 4
550 (2012) 1243-55.
551 53. C. I. Schroeder; J. E. Swedberg; D. J. Craik, Recent progress towards pharmaceutical
552 applications of disulfide-rich cyclic peptides. Curr Protein Pept Sci 14 (2013) 532-42.
553 54. M. L. Colgrave; D. J. Craik, Thermal, chemical, and enzymatic stability of the cyclotide
554 kalata B1: the importance of the cyclic cystine knot. Biochemistry 43 (2004) 5965-75.
555 55. C. T. Wong; D. K. Rowlands; C. H. Wong; T. W. Lo; G. K. Nguyen; H. Y. Li; J. P. Tam,
556 Orally active peptidic bradykinin B1 receptor antagonists engineered from a cyclotide scaffold for
557 inflammatory pain treatment. Angew Chem Int Ed Engl 51 (2012) 5620-4.
558 56. J. Rautio; H. Kumpulainen; T. Heimbach; R. Oliyai; D. Oh; T. Jarvinen; J. Savolainen,
559 Prodrugs: design and clinical applications. Nat Rev Drug Discov 7 (2008) 255-70.

560
561

FIGURE LEGENDS

Figure 1: Amino acid sequences and/or structures of incretins, α-conotoxins and peptidomimetics. Amino acid sequences of GLP-1 and Ex-4 (A). Chemical structures of BMS21 and compound 1 (B). Secondary structures and primary sequences of α-conotoxins cVc1.1 (C) and pc16a (D), with α-helices shown in green and disulfide bonds in yellow. Peptide segments not present in the naturally occurring α-conotoxins are shown in blue. Grafting points are indicated by scissors/dashed lines and the direction of the grafted segments are indicated by dashed arrows from the C-terminus to the N-terminus. (E) Structures of non-natural amino acids used for synthesis of peptidomimetic α-conotoxin chimeras.

Figure 2: Representative simulation structures calculated by molecular dynamics simulations. Representative simulation structures of compound 1 (A), compound 2 (B), compound 3 (C), compound 10 (D), compound 21 (E) and compound 27 (F), with the left-hand side of each panel showing atom stick models (carbon: green; nitrogen: blue; oxygen: red; sulphur: yellow; fluorine: white) and the right-hand side of each panel showing the secondary structures (α-helix: green; random coil: grey) and disulfide bonds in ball and stick model (carbon: green, sulphur: yellow).

Figure 3: Structures of compound 1 analogues with cysteine perfluoroarylation linkages. The structures of compound 1 analogues with varying cysteine perfluoroarylation linkages are shown for compound 27 (A), compound 28 (B) and compound 29 (C).

FIGURES

Figure 1

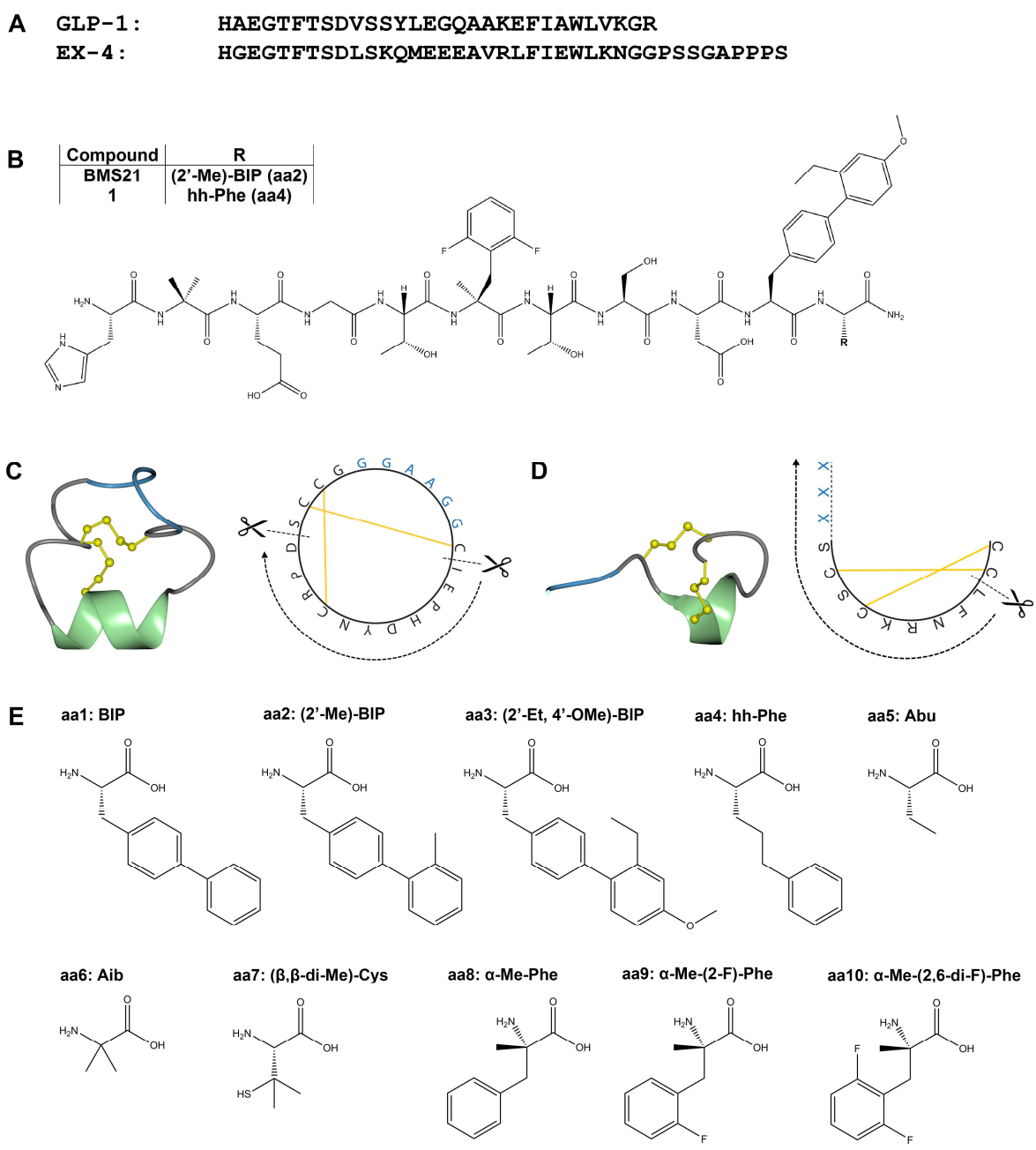

Figure 2

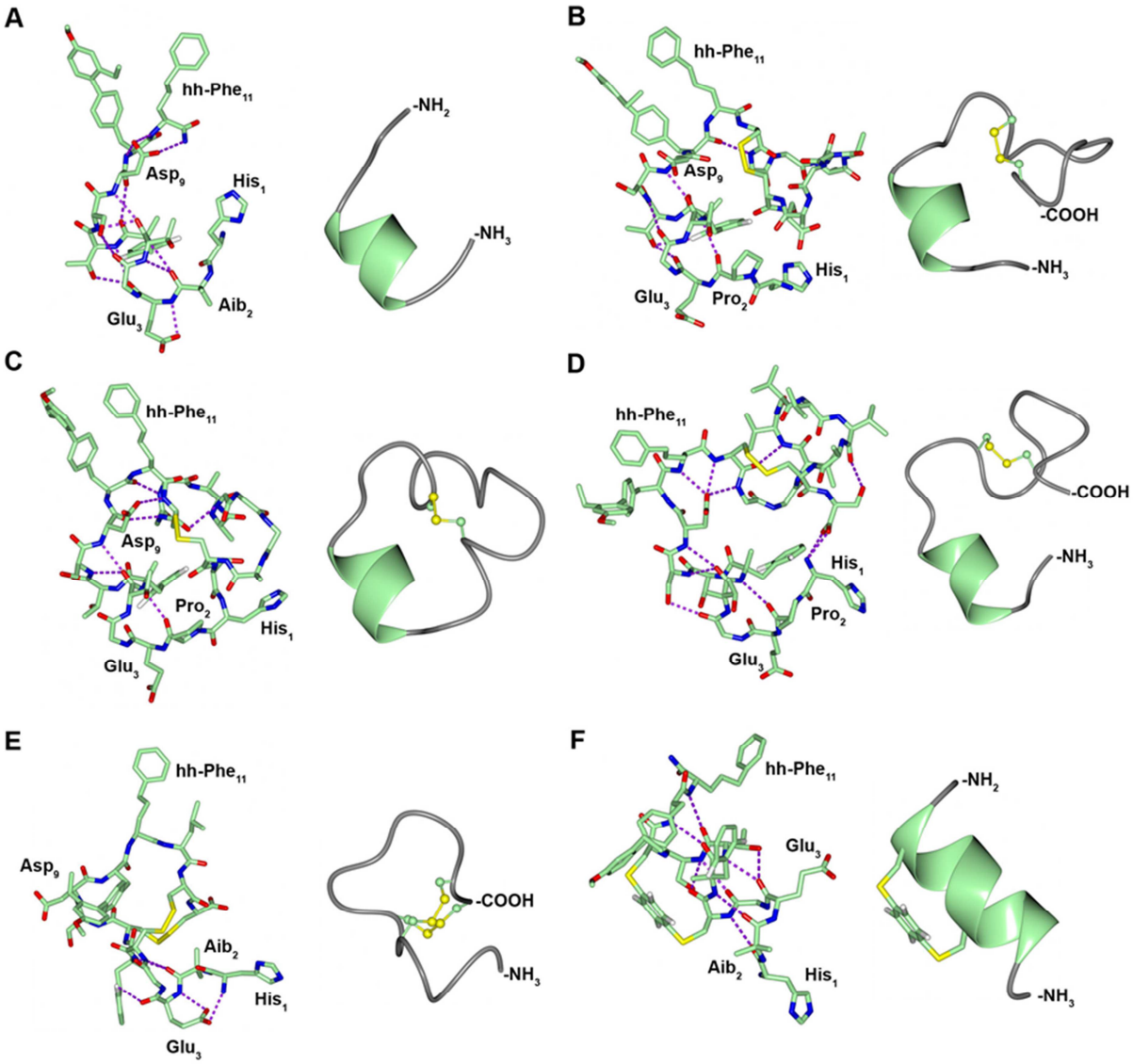

Figure 3

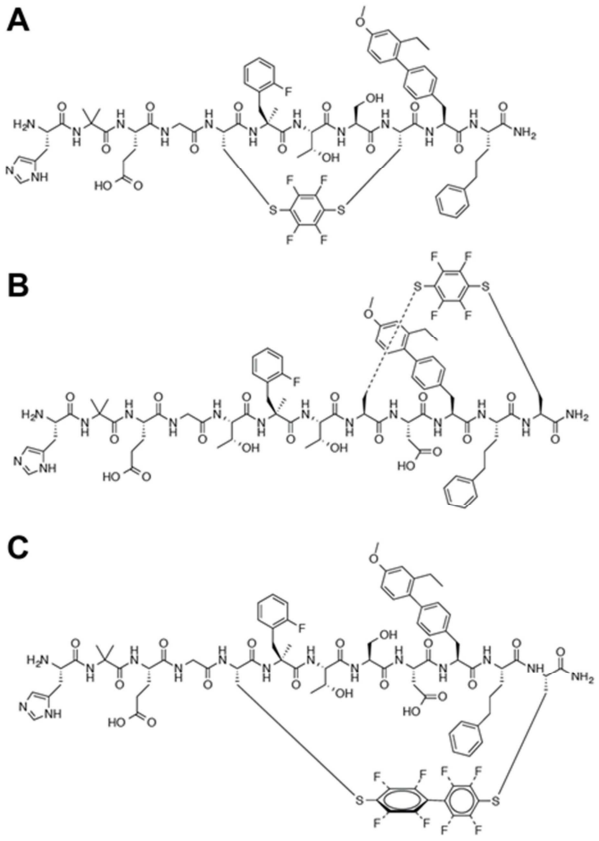

TABLES

Table 1: Sequences of α-conotoxins and grafted peptidomimetic chimeras

Residue[a]/ Compound	1	2	3	4	5	6	7	8	9	10	11	12	13	14	15	16	17	18	19	20	21	22	Modification[b]
α-conotoxin Vc1.1 and peptidomimetic chimeras[c]																							
cVc1.1	Asp	Pro	Arg	Cys	Asn	Tyr	Asp	His	Pro	Glu	Ile	Cys	Gly	Gly	Ala	Ala	Gly	Gly	Gly	Cys	Cys	Ser	Cyclo
2	His	Pro	Glu	Gly	Thr	**aa10**	Thr	Ser	Asp	**aa3**	**aa4**	Cys	Gly	Gly	Ala	Ala	Gly	Gly	Gly	Ala	Cys	Ser	-
3	His	Pro	Glu	Gly	Thr	**aa10**	Thr	Ser	Asp	**aa3**	**aa4**	Cys	Gly	Gly	Ala	Ala	Gly	Gly	Gly	Ala	Cys	Ser	Cyclo
4	His	**aa6**	Glu	Gly	Thr	**aa10**	Thr	Ser	Asp	**aa3**	**aa4**	Cys	Gly	Gly	Ala	Ala	Gly	Gly	Gly	Ala	Cys	Ser	Cyclo
5	His	Pro	Glu	Gly	Thr	**aa10**	Thr	Ser	Asp	**aa3**	**aa4**	Cys	Gly	Gly	Ala	Ala	Gly	Gly	Gly	Ala	Cys	Ser	Ac-
6	His	Pro	Glu	Gly	Thr	**aa9**	Thr	Ser	Asp	**aa3**	**aa4**	Cys	Gly	Gly	Ala	Ala	Gly	Gly	Gly	Ala	Cys	Ser	-
7	His	Pro	Glu	Gly	Thr	**aa9**	Thr	Ser	Asp	**aa3**	**aa4**	Cys	Gly	Gly	Ala	Ala	Gly	Gly	Gly	Ala	Cys	Ser	Cyclo
8	His	Pro	Glu	Gly	Thr	**aa8**	Thr	Ser	Asp	**aa3**	**aa4**	Cys	Gly	Gly	Ala	Ala	Gly	Gly	Gly	Ala	Cys	Ser	Cyclo
9	His	Pro	Glu	Gly	Thr	Phe	Thr	Ser	Asp	**aa3**	**aa4**	Cys	Gly	Gly	Ala	Ala	Gly	Gly	Gly	Ala	Cys	Ser	Cyclo
10	His	Pro	Glu	Gly	Thr	**aa10**	Thr	Ser	Asp	**aa3**	**aa4**	Cys	Gly	Gly	Val	Val	Val	Gly	Val	Val	Cys	Ser	-
11	His	Pro	Glu	Gly	Thr	**aa10**	Thr	Ser	Asp	**aa3**	**aa4**	Cys	Gly	Gly	Val	Val	Val	Gly	Val	Val	Cys	Ser	Cyclo
12	His	Pro	Glu	Gly	Thr	**aa8**	Thr	Ser	Asp	**aa3**	**aa4**	Cys	Gly	Gly	Leu	Leu	Leu	Gly	Leu	Leu	Cys	Ser	-
13	His	Pro	Glu	Gly	Thr	**aa8**	Thr	Ser	Asp	**aa3**	**aa4**	Cys	Gly	Gly	Leu	Leu	Leu	Gly	Leu	Leu	Cys	Ser	Cyclo
14	His	Pro	Glu	Gly	Thr	**aa10**	Thr	Ser	Asp	**aa3**	**aa4**	Cys	Gly	**aa1**	Ala	Ala	Gly	Gly	Gly	Ala	Cys	Ser	-
15	His	Pro	Glu	Gly	Thr	**aa10**	Thr	Ser	Asp	**aa3**	**aa4**	Cys	Gly	**aa1**	Ala	Ala	Gly	Gly	Gly	Ala	Cys	Ser	Cyclo
16	His	Pro	Glu	Gly	Thr	**aa8**	Thr	Ser	Asp	**aa3**	**aa4**	Cys	Gly	**aa1**	Ala	Ala	Gly	Gly	Gly	Ala	Cys	Ser	-
17	His	Pro	Glu	Gly	Thr	**aa8**	Thr	Ser	Asp	**aa3**	**aa4**	Cys	Gly	**aa1**	Ala	Ala	Gly	Gly	Gly	Ala	Cys	Ser	Cyclo
18	His	Pro	Glu	Gly	Thr	**aa10**	Thr	Ser	Asp	**aa3**	**aa4**	**aa7**	Gly	Gly	Ala	Ala	Gly	Gly	Gly	Ala	**aa7**	Ser	-
19	His	Pro	Glu	Gly	Thr	**aa10**	Thr	Ser	Asp	**aa3**	**aa4**	**aa7**	Gly	Gly	Ala	Ala	Gly	Gly	Gly	Ala	**aa7**	Ser	Cyclo
20	His	Pro	Glu	Gly	Thr	**aa10**	Thr	Ser	Asp	**aa3**	**aa4**	**aa5**	Gly	Gly	Ala	Ala	Gly	Gly	Gly	Ala	**aa5**	Ser	-
α-conotoxin pc16a and peptidomimetic chimeras[c]																							
pc16a	-	-	-	Ser	Cys	Ser	Cys	Lys	Arg	**Asn**	**Phe**	Leu	Cys	Cys	-	-	-	-	-	-	-	-	-NH_2
21	His	**aa6**	Glu	Gly	Cys	**aa10**	Cys	Ser	Asp	**aa3**	**aa4**	Leu	Cys	Cys	-	-	-		-	-	-	-	-
22	His	**aa6**	Glu	Gly	Cys	**aa9**	Cys	Ser	Asp	**aa3**	**aa4**	Leu	Cys	Cys	-	-	-		-	-	-	-	-
23	His	**aa6**	Glu	Gly	Cys	**aa8**	Cys	Ser	Asp	**aa3**	**aa4**	Leu	Cys	Cys	-	-	-		-	-	-	-	-
24	His	**aa6**	Glu	Gly	Cys	Phe	Cys	Ser	Asp	**aa3**	**aa4**	Leu	Cys	Cys	-	-	-		-	-	-	-	-
25	His	**aa6**	Glu	Gly	Cys	**aa10**	Cys	Ser	Asp	**aa3**	**aa4**	Leu	Cys	Cys	-	-	-		-	-	-	-	Ac-
26	His	**aa6**	Glu	Gly	Cys	**aa10**	Cys	Ser	Asp	**aa3**	**aa4**	**aa1**	Cys	Cys	-	-	-		-	-	-	-	-
helix-constrained compound 1 analogues																							
27	His	**aa6**	Glu	Gly	Cys	**aa9**	Thr	Ser	Cys	**aa3**	**aa4**	-	-	-	-	-	-	-	-	-	-	-	-NH_2
28	His	**aa6**	Glu	Gly	Thr	**aa9**	Thr	Cys	Asp	**aa3**	**aa4**	Cys	-	-	-	-	-	-	-	-	-	-	-NH_2
29	His	**aa6**	Glu	Gly	Cys	**aa9**	Thr	Ser	Asp	**aa3**	**aa4**	Cys	-	-	-	-	-	-	-	-	-	-	-NH_2

[a]Non-canonical amino acids are referred to as aaX (where X is a number) and their molecular structures are shown in figure 1E

[b]Modifications**:** Cyclo, peptide backbone cyclization; dash (-), uncyclized peptide backbone; -NH_2, amidated C-terminus of peptide; Ac, acetylated N-terminus of peptide

[c]Black lines indicate disulfide connectivity.

Table 2: Masses and cAMP activities (CHO-GLP-1 cells) of grafted α-conotoxins and peptidomimetic chimeras

Compound	Calculated mass (Da)	Determined mass (Da)	cAMP EC_{50} (nM) ± SEM	n
1	1482.6	1483.2	0.14 ± 0.01	3
2	2285.8	2285.8	0.85 ± 0.07	3
3	2267.9	2268.6	430 ± 40	3
4	2257.4	2257.2	1400 ± 50	3
5	2327.0	2327.7	13 ± 0.5	3
6	2267.9	2268.1	1.0 ± 0.4	3
7	2250.6	2249.9	1000 ± 30	3
8	2231.9	2231.8	2000 ± 100	3
9	2217.9	2219.9	390 ± 40	3
10	2453.8	2453.1	19 ± 0.5	3
11	2435.8	2437.0	1000 ± 100	3
12	2470.9	2471.0	130 ± 40	3
13	2488.0	2488.5	2800 ± 130	3
14	2451.1	2452.0	2.4 ± 0.06	3
15	2433.1	2434.8	470 ± 20	3
16	2399.0	2399.0	47 ± 2	3
17	2415.8	2415.5	360 ± 10	3
18	2342.6	2342.2	2.5 ± 0.2	3
19	2324.6	2325.9	2000 ± 50	3
20	2251.5	2251.8	0.47 ± 0.02	3
21	1803.4	1803.5	430 ± 80	3
22	1784.0	1784.3	5000 ± 1000	3
23	1766.7	1767.5	1600 ± 50	3
24	1752.6	1753.4	16000 ± 700	3
25	1844.9	1846.5	69 ± 27	3
26	1914.0	1914.6	7500 ± 1100	3
27	1600.6	1600.7	850 ± 45	3
28	1729.6	1729.8	1150 ± 50	2
29	1863.6	1863.7	>1000	1

Table 3: Biophysical parameters calculated from molecular dynamics

Compound	R_g (Å)	PSA (Å^2)	SA (Å^2)	vLogP
1	8.2 ± 0.3	492 ± 30	1736 ± 36	0.39 ± 0.04
2	7.9 ± 0.1	651 ± 32	2138 ± 67	-2.24 ± 0.07
3	7.8 ± 0.1	636 ± 39	2026 ± 42	-1.16 ± 0.04
10	7.9 ± 0.1	543 ± 30	2227 ± 48	3.22 ± 0.34
11	7.8 ± 0.1	512 ± 18	2213 ± 31	3.76 ± 0.33
20	8.3 ± 0.2	715 ± 26	2377 ± 47	-3.30 ± 0.32
21	7.1 ± 0.2	577 ± 28	1786 ± 42	0.20 ± 0.06
25	7.2 ± 0.1	514 ± 25	1831 ± 52	3.14 ± 0.36
27	7.2 ± 0.2	444 ± 21	1654 ± 44	3.94 ± 0.40

SUPPLEMENTARY INFORMATION

Cyclic alpha-Conotoxin Peptidomimetic Chimeras as Potent GLP-1R Agonists.

Joakim E. Swedberg[a], Christina I. Schroeder[a], Justin Mitchell[a], Thomas Durek[a], David P. Fairlie[a], David J. Edmonds[b], David A. Griffith[b], Roger B. Ruggeri[b], David R. Derksen[c], Paula M. Loria[c], Spiros Liras[b], David A. Price[b], and David J. Craik[a,*]

[a]Institute for Molecular Bioscience, The University of Queensland, Brisbane, 4072 QLD, Australia

[b]World Wide Medicinal Chemistry, CVMED, Pfizer Inc., Cambridge, Massachusetts, USA

[c]Pharmacokinetics, Dynamics and Metabolism, Worldwide Research & Development, Pfizer Inc., Groton, Connecticut, USA

*Corresponding author Address: Institute for Molecular Bioscience, The University of Queensland, Brisbane QLD 4072, Australia; Phone: +61 (0)7 3346 2019; Email: d.craik@imb.uq.edu.au.

CONTENTS

Figure S1: ^{1}H NMR spectra of representative peptides included in this work
^{1}H NMR spectra of compounds 2, 3, 4 and 5 2
^{1}H NMR spectra of compounds 7, 8, 9 and 10 3
^{1}H NMR spectra of compounds 11, 12, 15 and 16 4
^{1}H NMR spectra of compounds 17, 18, 19 and 20 5
^{1}H NMR spectra of compounds 21, 23, 25 and 26 6
Figure S2: Secondary structure analysis from molecular dynamics trajectories
Secondary structure analysis: secondary structure color code key 7
Secondary structure analysis: compound 1 7
Secondary structure analysis: compound 2 8
Secondary structure analysis: compound 3 9
Secondary structure analysis: compound 10 10
Secondary structure analysis: compound 11 11
Secondary structure analysis: compound 20 12
Secondary structure analysis: compound 21 13
Secondary structure analysis: compound 25 14
Secondary structure analysis: compound 27 15

Figure S1: **^{1}H NMR spectra of peptides used in this study**. Experiments were run on a Bruker 600 MHz Avance spectrometer at 298K in 12-60% ACN-d3 / H_2O.

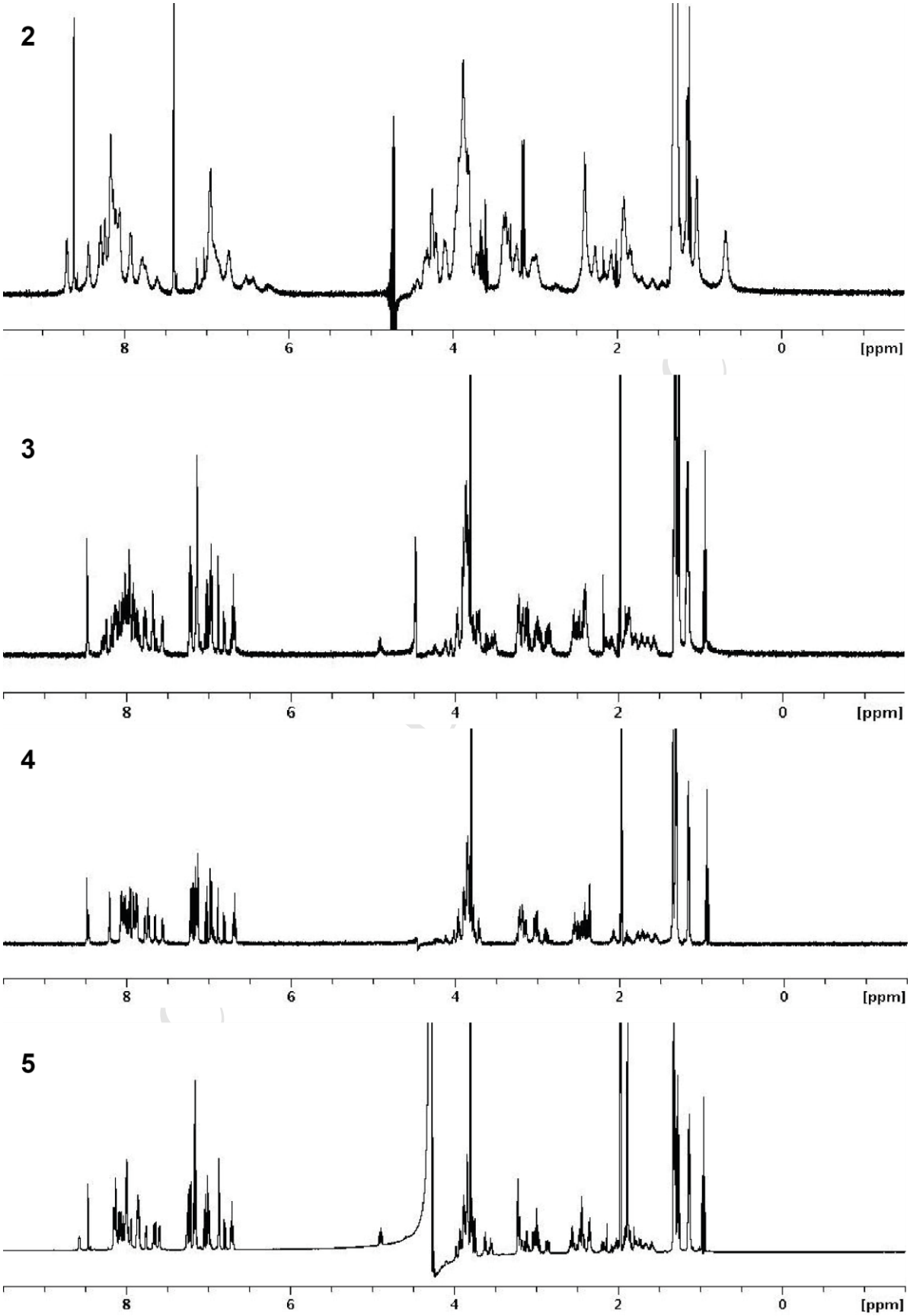

Figure S1: **^{1}H NMR spectra of peptides used in this study (continued).**

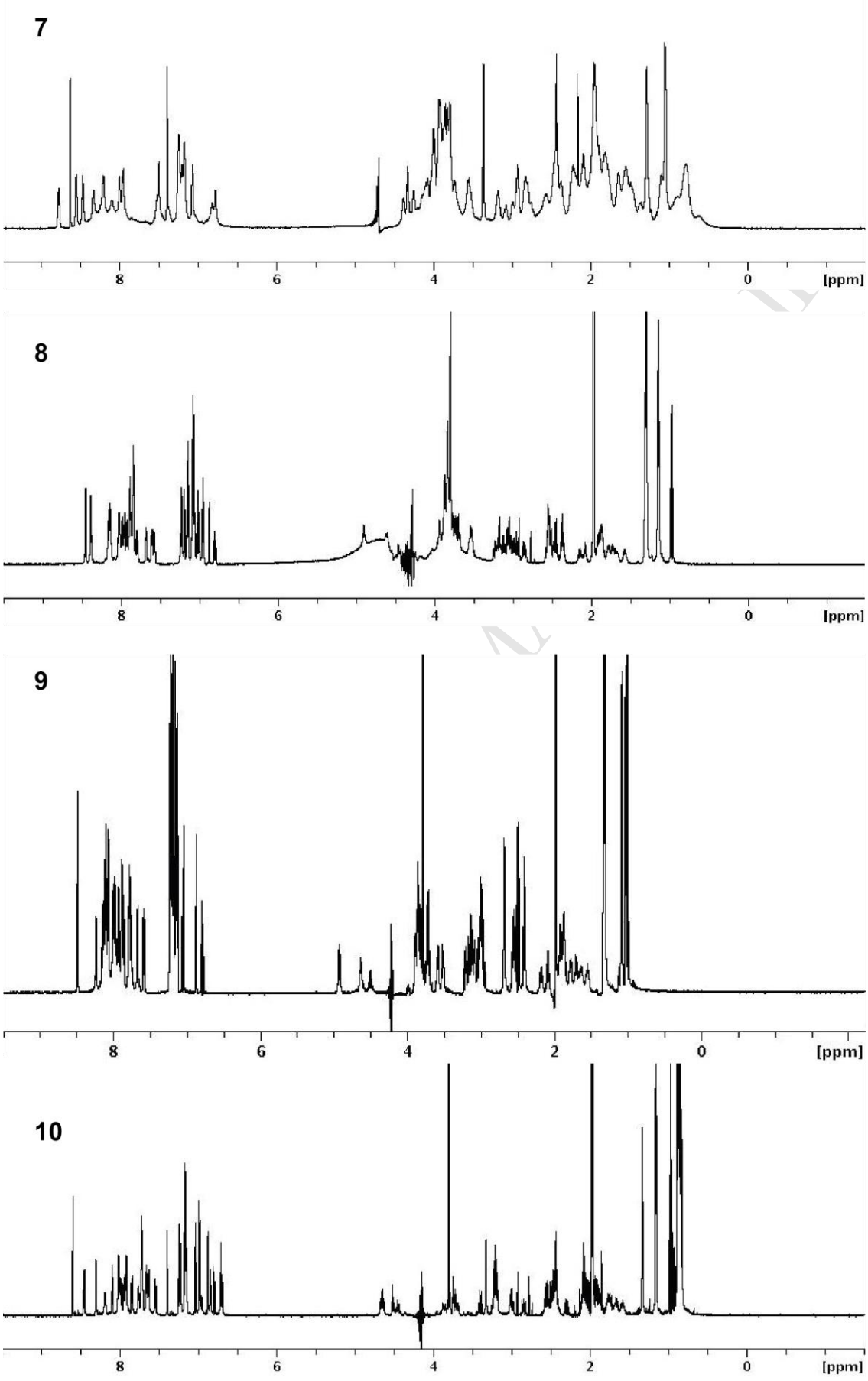

Figure S1: **^{1}H NMR spectra of peptides used in this study (continued).**

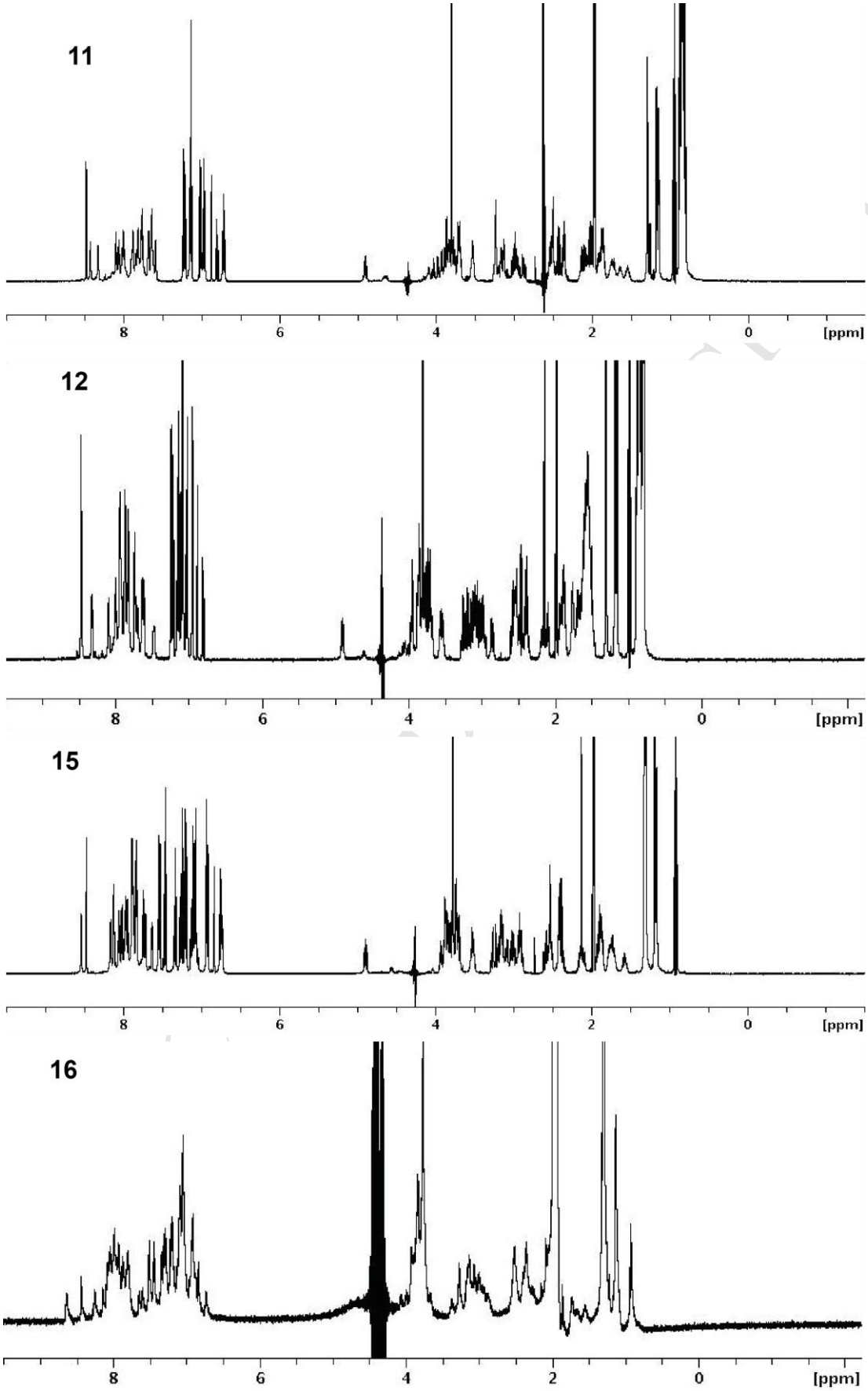

Figure S1: **^{1}H NMR spectra of peptides used in this study (continued).**

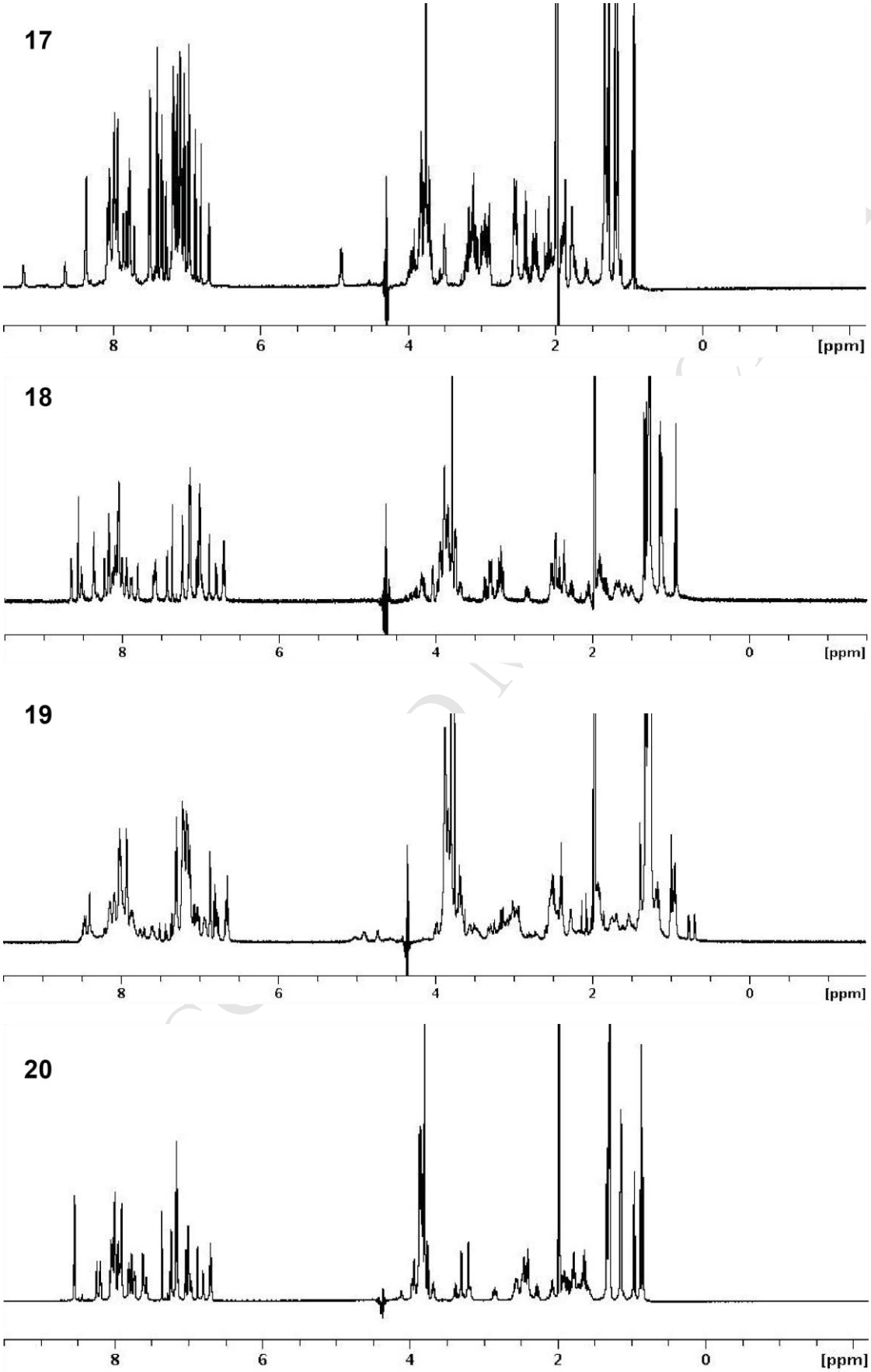

Figure S1: **^{1}H NMR spectra of peptides used in this study (continued).**

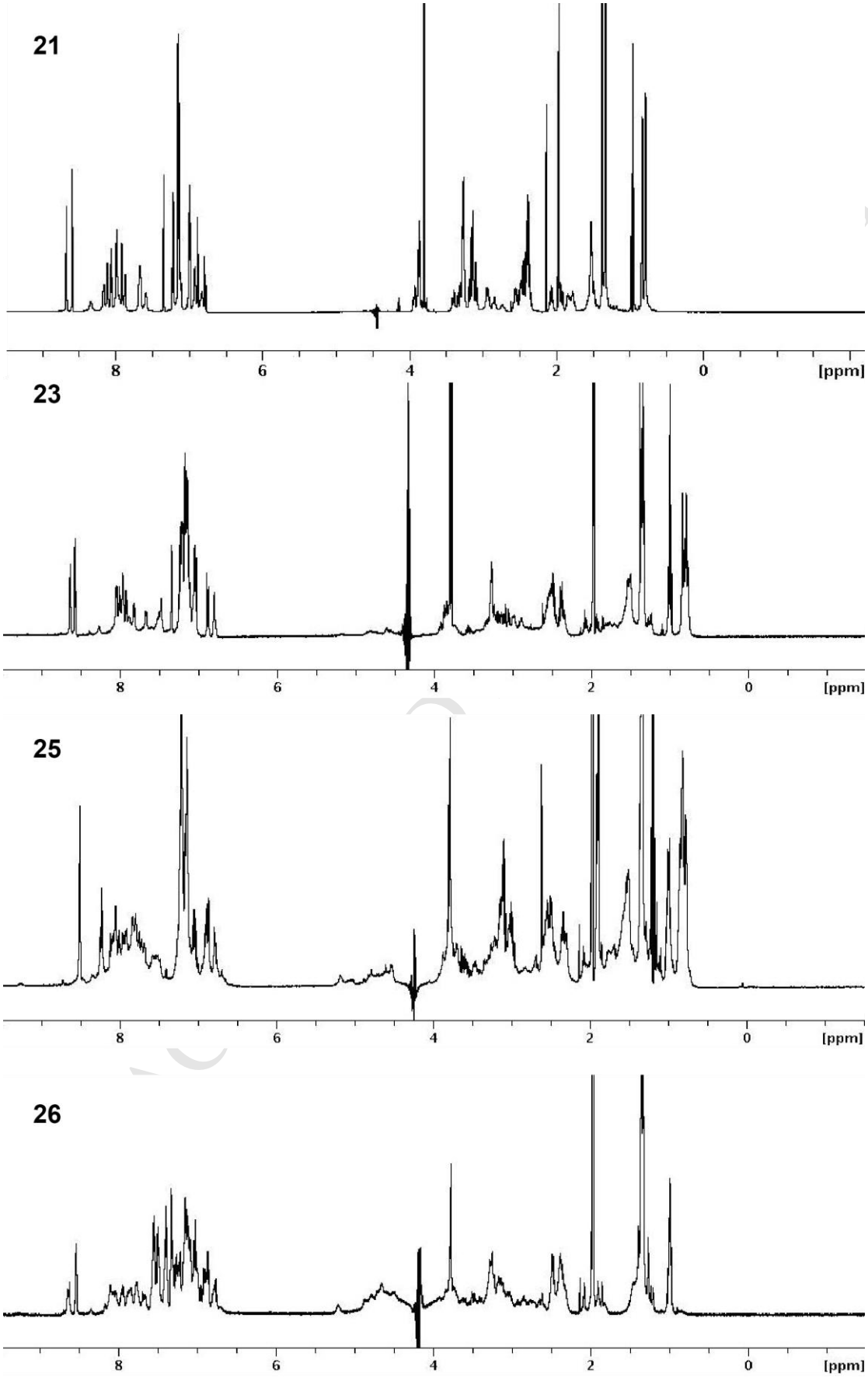

Figure S2: Secondary structure analysis from molecular dynamics trajectories. Plots of calculated secondary structures during molecular dynamics simulations over time (x-axis) versus peptidomimetic residue number (y-axis) for three replicates of 50 ns simulations (top to bottom). A secondary structure color code key is given below.

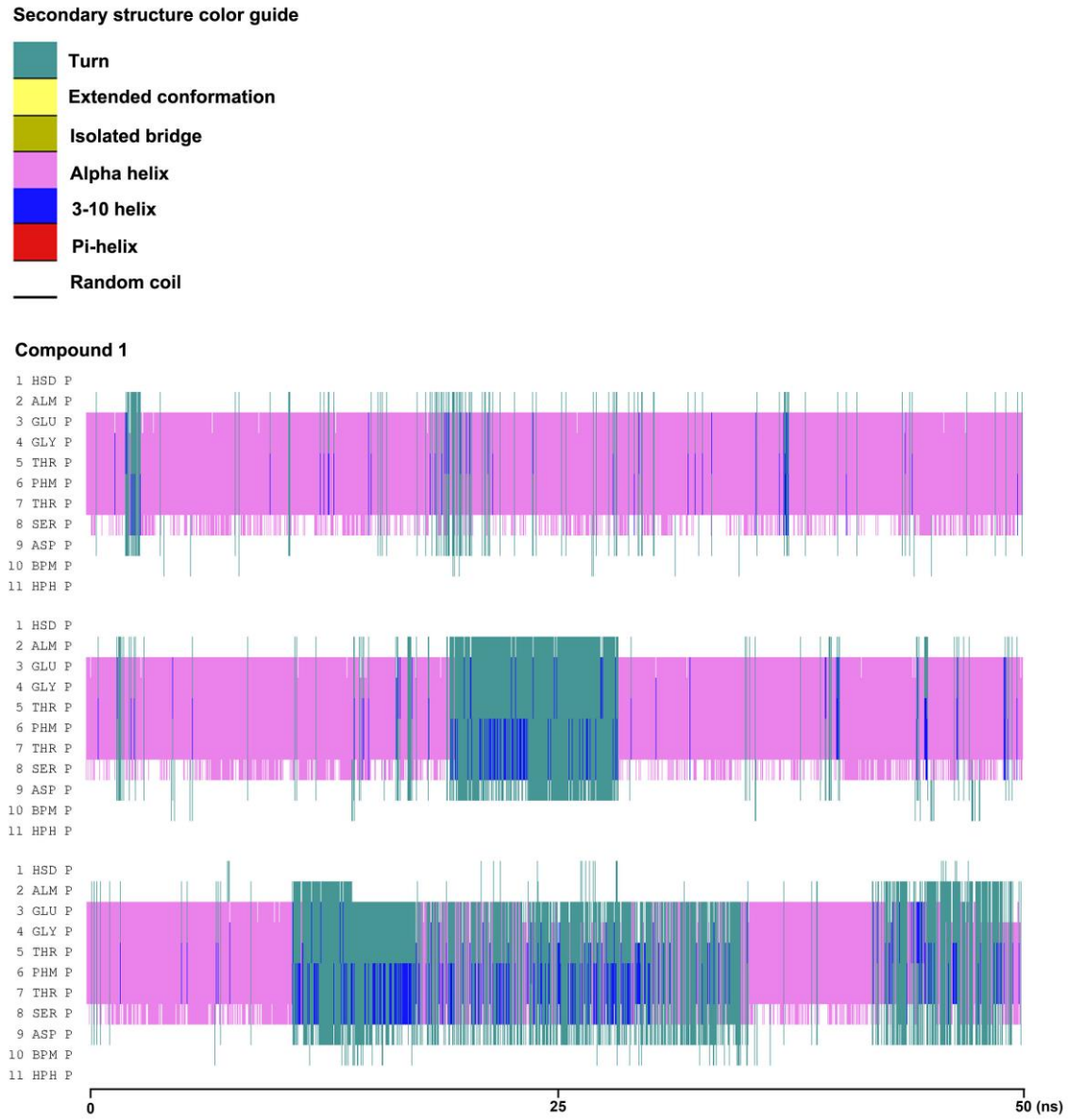

Figure S2: Secondary structure analysis from molecular dynamics trajectories (continued)

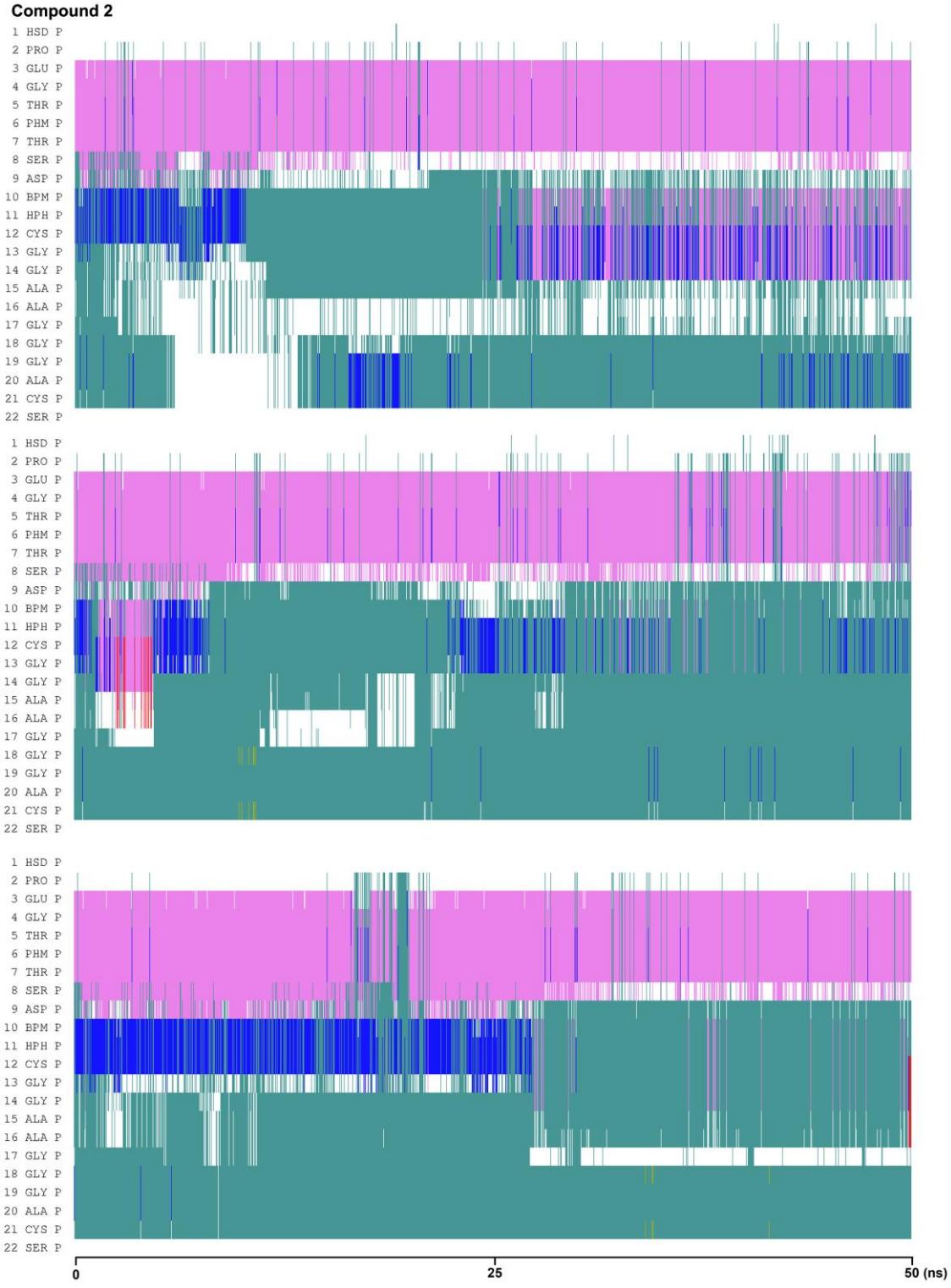

Figure S2: Secondary structure analysis from molecular dynamics trajectories (continued)

Figure S2: Secondary structure analysis from molecular dynamics trajectories (continued)

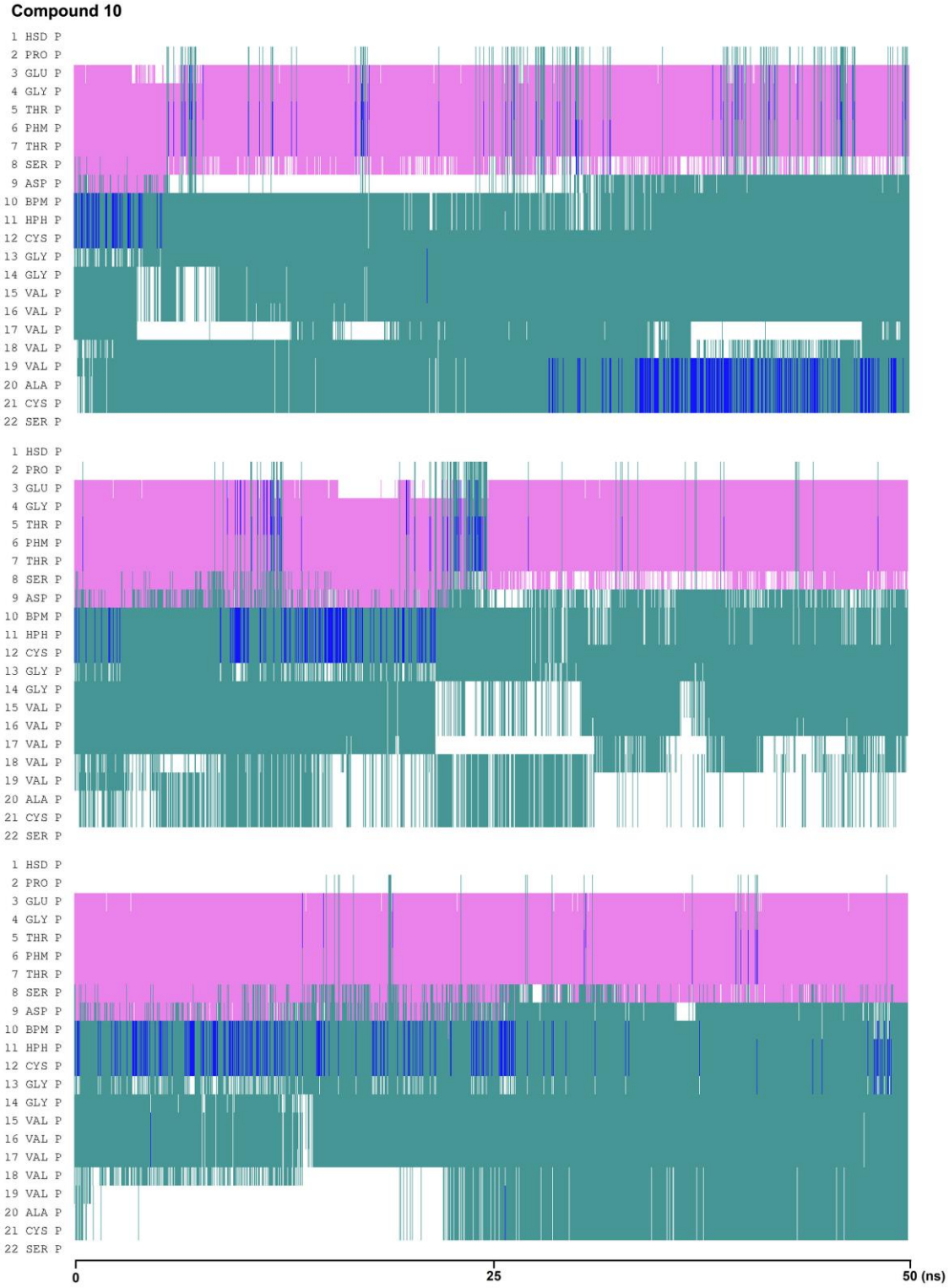

Figure S2: Secondary structure analysis from molecular dynamics trajectories (continued)

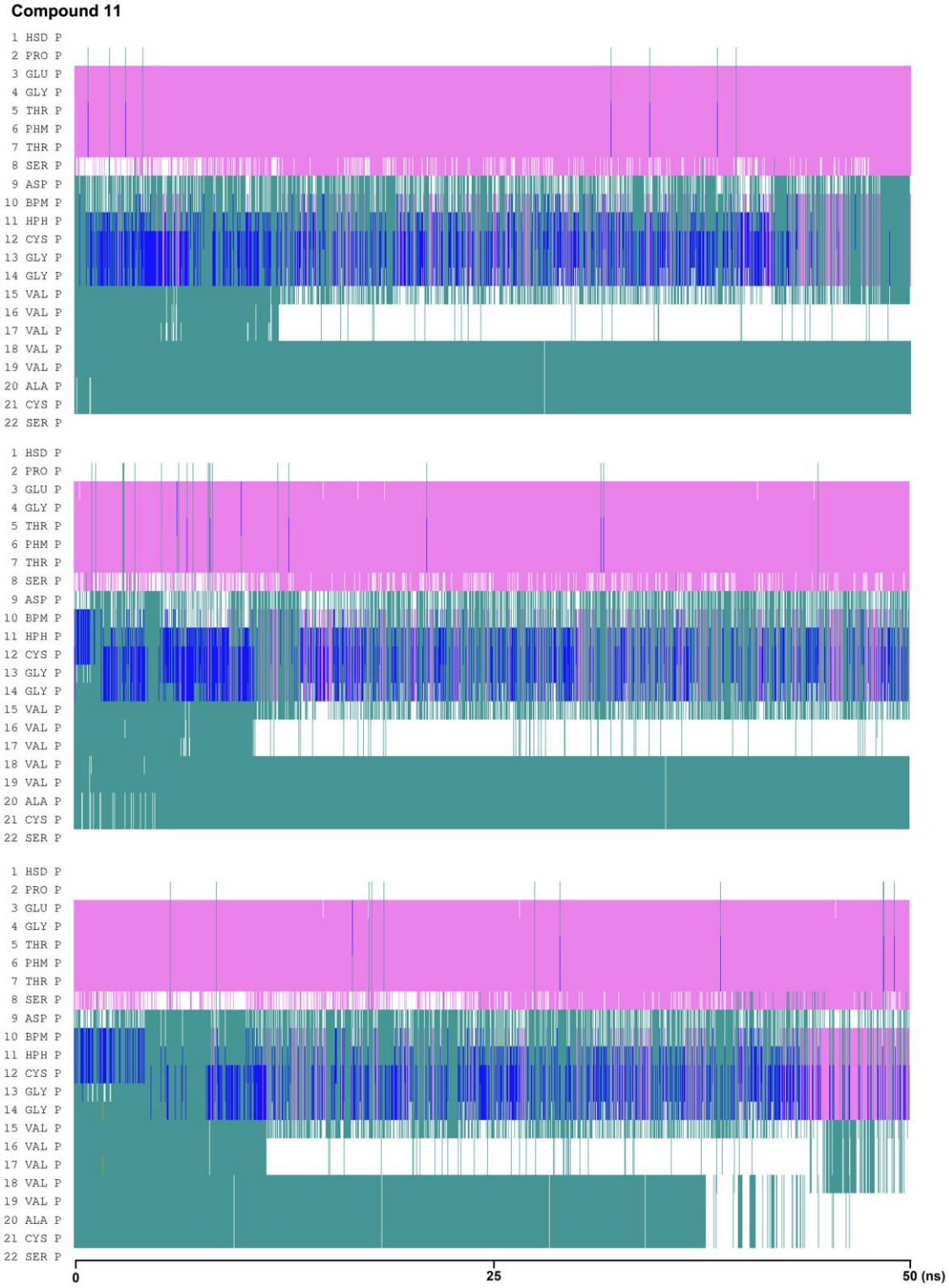

Figure S2: Secondary structure analysis from molecular dynamics trajectories (continued)

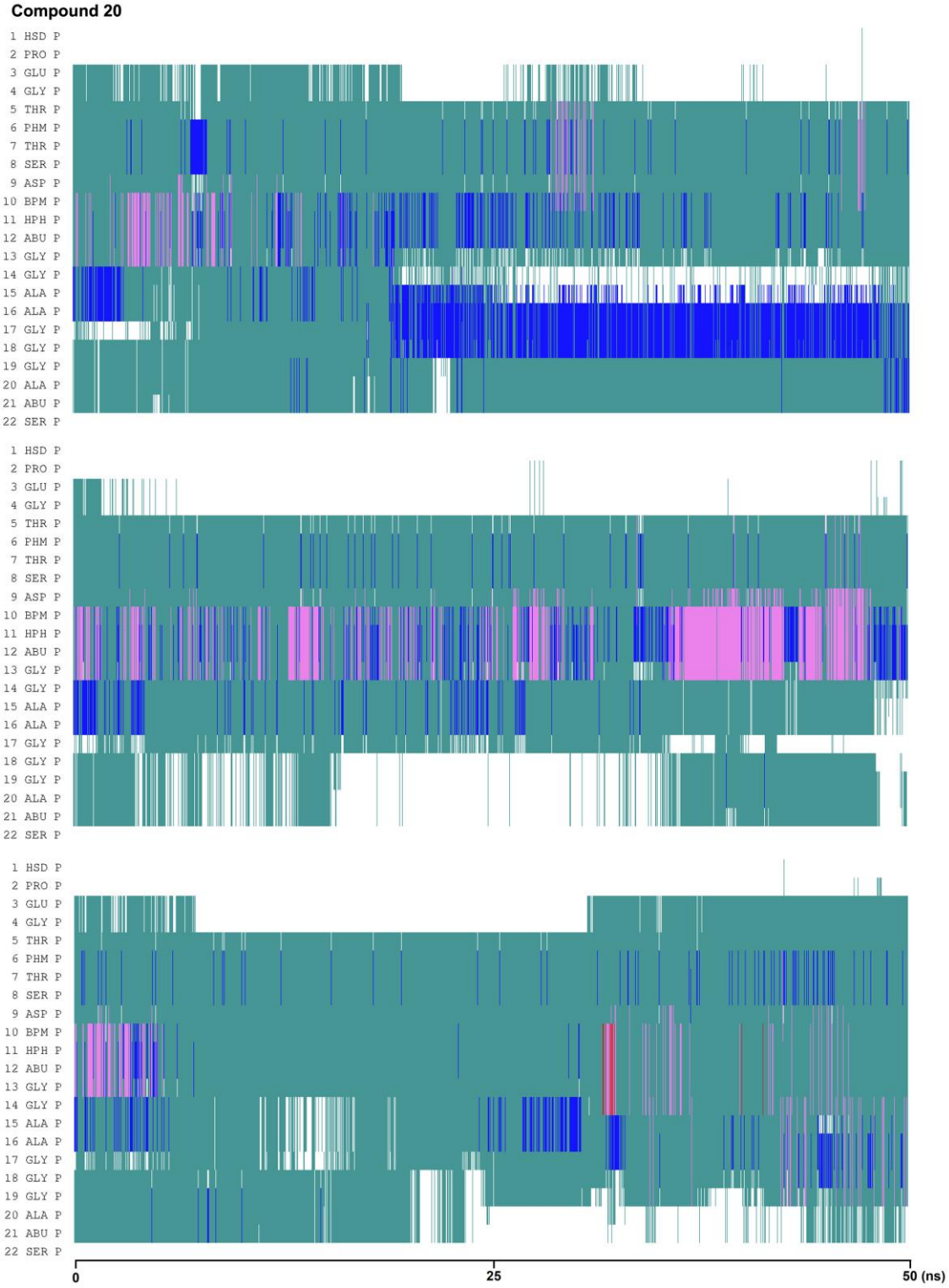

Figure S2: Secondary structure analysis from molecular dynamics trajectories (continued)

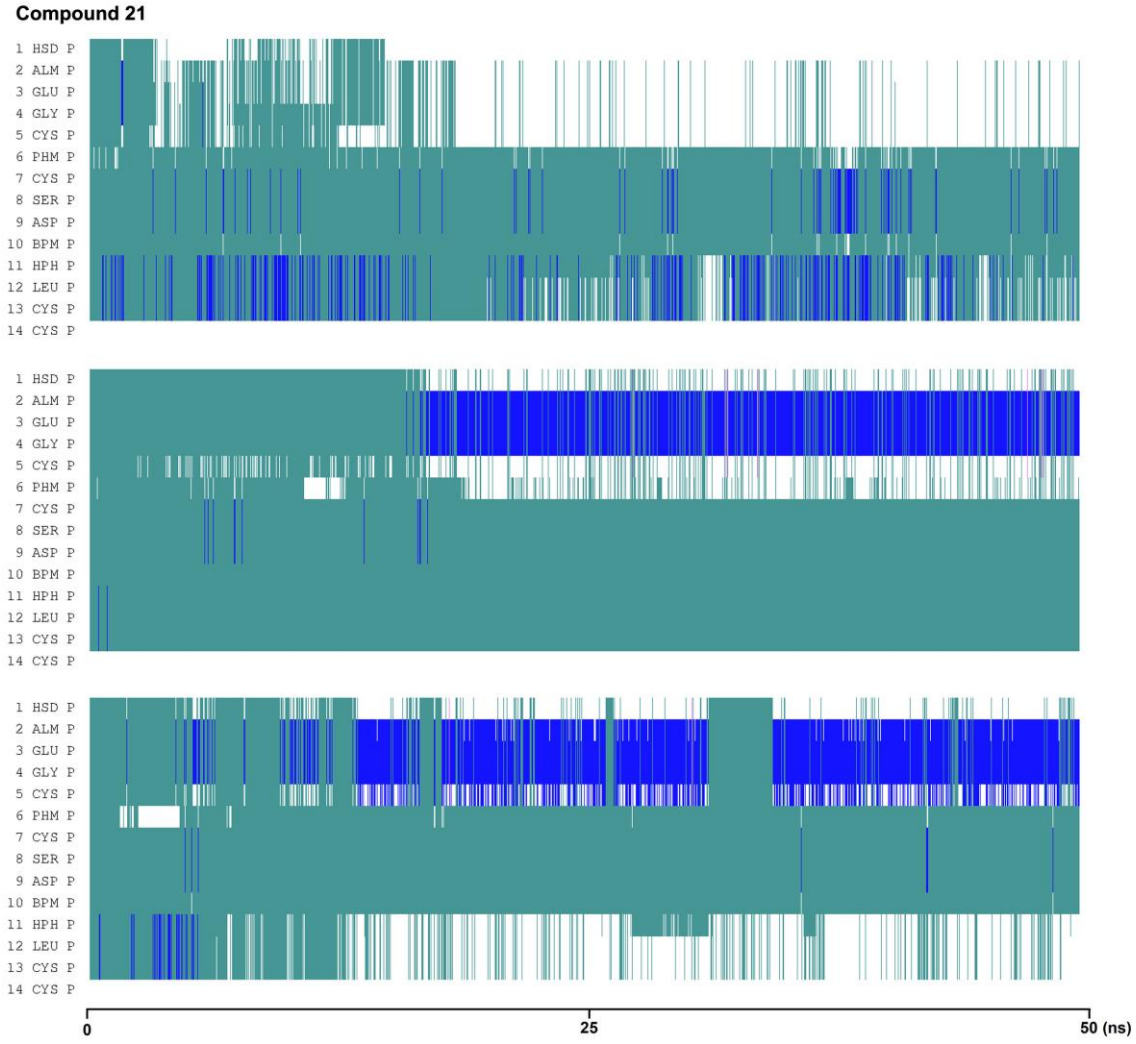

Figure S2: Secondary structure analysis from molecular dynamics trajectories (continued)

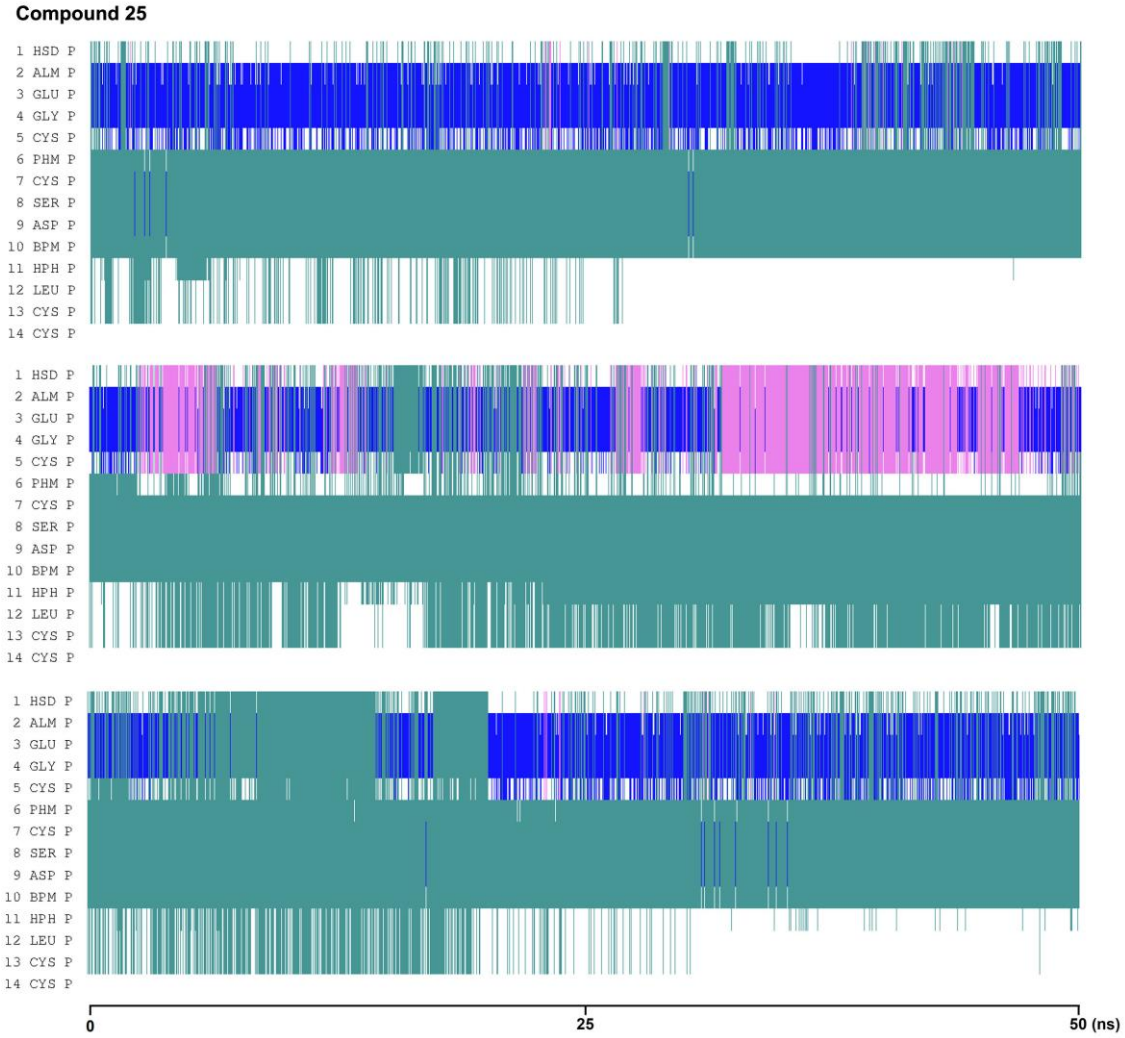

Figure S2: Secondary structure analysis from molecular dynamics trajectories (continued)